

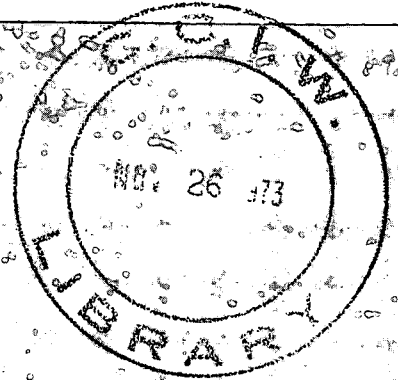


Environment
Canada

Environnement
Canada

The Effect of Impurities on the Mechanical Properties of Ice Single Crystals

T. Nakamura and S. J. Jones



GB
707
C335
no. 24

SCIENTIFIC SERIES NO. 24

**INLAND WATERS DIRECTORATE,
WATER RESOURCES BRANCH,
OTTAWA, CANADA, 1973.**



Environment
Canada

Environnement
Canada

The Effect of Impurities on the Mechanical Properties of Ice Single Crystals

T. Nakamura and S. J. Jones

SCIENTIFIC SERIES NO. 24

*INLAND WATERS DIRECTORATE,
WATER RESOURCES BRANCH,
OTTAWA, CANADA, 1973.*

©
Information Canada
Ottawa, 1973

Cat. No.: En 36-502/24

CONTRACT #02KXKL327-3-8060
THORN PRESS LIMITED

Contents

	Page
ABSTRACT	vii
INTRODUCTION	1
EXPERIMENTAL	1
Preparation of crystals	1
Procedures	1
RESULTS	2
General results	2
HF-doped crystals	2
HCl-doped crystals	3
H ₂ O ₂ -doped crystals	3
NH ₄ OH-doped crystals	3
HBr-doped crystals	3
NH ₄ F-doped crystals	3
NaF-doped crystals	3
KF-doped crystals	3
NaOH-doped crystals	3
He-doped crystals	3
Dependence of strain-rate on stress	3
Activation energy of pure and HCl-doped crystals	4
Distribution of ions in single crystals	4
CONCLUSIONS AND DISCUSSION	5
ACKNOWLEDGMENTS	5
REFERENCES	6
APPENDIX (Figures 2 to 45)	7

Illustrations

Figure 1. Basal slip lines on an NaOH-doped single crystal of ice deformed 20% at -26°C	2
Figure 2. Stress-strain curves for pure and HF-doped ice deformed at -11°C and various strain-rates and dopant concentrations as marked on the figure ...	9
Figure 3. Maximum resolved shear stress plotted against strain-rate for pure and HF-doped ice at -11°C. The number beside each filled circle is the HF concentration, in ppm, of the sample	9
Figure 4. Stress-strain curves for HF-doped ice deformed at -30°C and various strain-rates as marked on the figure	10

Illustrations (cont'd)

	Page
Figure 5. Stress-strain curves for HF-doped ice deformed at -30°C and various strain-rates as marked on the figure	10
Figure 6. A stress-strain curve of one pure ice crystal deformed at -31°C at a strain-rate of $9.3 \times 10^{-7} \text{ s}^{-1}$	11
Figure 7. Maximum resolved shear stress plotted against strain-rate for pure and HF-doped ice deformed at -30°C . The number beside each filled circle is the HF concentration of the sample, in ppm	11
Figure 8. Stress-strain curves for pure and HF-doped ice deformed at -26°C and various strain-rates and dopant concentrations as on the figure	12
Figure 9. Stress-strain curves for pure and HCl-doped ice deformed at -26°C at a strain-rate of $4 \times 10^{-7} \text{ s}^{-1}$	12
Figure 10. Stress-strain curves for pure and HCl-doped ice deformed at -26°C at a strain-rate of $1.6 \times 10^{-6} \text{ s}^{-1}$	13
Figure 11. Stress-strain curves for pure and HCl-doped ice deformed at -26°C at a strain-rate of $4 \times 10^{-6} \text{ s}^{-1}$	13
Figure 12. Stress-strain curve for HCl-doped ice deformed at -26°C at a strain-rate of $4.4 \times 10^{-6} \text{ s}^{-1}$	14
Figure 13. Maximum resolved shear stress plotted against strain-rate for pure and HCl-doped ice deformed at -26°C . The number beside each filled circle is the HCl concentration of the sample in ppm	14
Figure 14. Stress-strain curves of pure and HCl-doped ice deformed at -46°C at various strain-rates as marked on the figure	15
Figure 15. Maximum resolved shear stress plotted against strain-rate for pure and HCl-doped ice deformed at -46°C . The number beside each filled circle is the HCl concentration of the sample, in ppm	15
Figure 16. Stress-strain curves for pure and HCl-doped ice deformed at -15°C at various strain-rates and dopant concentrations as marked on the figure ...	16
Figure 17. Stress-strain curves for pure and HCl-doped ice deformed at -15°C at various strain-rates as marked on the figure	16
Figure 18. Maximum resolved shear stress plotted against strain-rate for pure, HCl-doped and He-doped ice at -15°C . The dopant concentration is marked for each sample	17
Figure 19. Stress-strain curves for pure and HCl-doped ice deformed at -5.6°C at various strain-rates as marked	17
Figure 20. Stress-strain curves for pure and HCl-doped ice deformed at -5.6°C at various strain-rates as marked	18
Figure 21. Maximum resolved shear stress plotted against strain-rate for pure and HCl-doped ice at -5.6°C . The number beside each filled circle is the HCl concentration in the sample, in ppm	18

Illustrations (cont'd)

	Page
Figure 22. Stress-strain curves for two H ₂ O ₂ -doped samples and two pure ice samples deformed at -26°C at a strain-rate of $4 \times 10^{-7} \text{ s}^{-1}$	19
Figure 23. Stress-strain curves for NH ₄ OH-doped ice deformed at -11.7°C at various strain-rates as marked	19
Figure 24. Maximum resolved shear stress plotted against strain-rate for pure and NH ₄ OH-doped ice at -11°C. The concentration of NH ₄ OH was about 0.1 ppm in the doped samples	20
Figure 25. Stress-strain curves for NH ₄ OH and pure ice deformed at -26°C at various strain-rates as marked	20
Figure 26. Stress-strain curves for HBr-doped ice deformed at -26°C at a strain-rate of $4.5 \times 10^{-6} \text{ s}^{-1}$	21
Figure 27. Stress-strain curves for pure and NaF-doped ice at -26°C at a strain-rate of $1.6 \times 10^{-6} \text{ s}^{-1}$	21
Figure 28. Stress-strain curves for one pure and one KF-doped sample deformed at -33°C and at a strain-rate of $8.5 \times 10^{-8} \text{ s}^{-1}$	22
Figure 29. Stress-strain curves for pure and NaOH-doped ice deformed at -26°C at various strain-rates as marked on the figure. The curve marked D(20°) was a sample with an angle of 20° between its optic and tensile axis	22
Figure 30. Maximum resolved shear stress plotted against strain-rate for pure and NaOH-doped ice at -26°C	23
Figure 31. Stress-strain curve for two He-doped ice crystals deformed at -15°C. After testing, one sample had no Helium left in it	23
Figure 32. Showing the variation of load with crosshead speed. Each line represents one sample deformed at different rates at various temperatures down to -53°C. The slope of each lines gives a stress exponent 'n' shown in the figure	24
Figure 33. Stress-strain curve for one HCl-doped specimen deformed at different temperatures at a strain-rate of $4.5 \times 10^{-7} \text{ s}^{-1}$	24
Figure 34. Stress-strain curve for one HCl-doped ice crystal deformed at different temperatures at a strain-rate of $8.2 \times 10^{-7} \text{ s}^{-1}$	25
Figure 35. Stress-strain curve for one HCl-doped specimen deformed at different temperatures at a strain-rate of $1.7 \times 10^{-6} \text{ s}^{-1}$	25
Figure 36. Stress-strain curve for HCl-doped specimen deformed at different temperatures at a strain-rate of $8.7 \times 10^{-6} \text{ s}^{-1}$. The sample was the same one as used for Figure 35	26
Figure 37. Determination of activation energy for HCl-doped crystals by comparison of stress immediately before and after changing temperatures. Samples used were those shown in Figures 33-36	26

Illustrations (cont'd)

	Page
Figure 38. Determination of activation energy for HCl-doped ice by comparing strain-rates required at different temperatures to give a constant maximum resolved shear stress. Stresses are shown for each line and the slope of the line is proportional to the activation energy	27
Figure 39. Determination of activation energy for pure ice by comparing strain-rates required at different temperatures to give a constant maximum resolved shear stress. Stresses are shown for each line and the slope of the line is proportional to the activation energy	27
Figure 40. Maximum resolved shear stress for all pure and HCl-doped samples plotted against strain-rate reduced to -26°C by using an activation energy of 18 kcal/mole for pure ice and 13 kcal/mole for HCl-doped ice	28
Figure 41. Radial distribution of fluoride in a cylindrical single crystal of HF-doped ice	28
Figure 42. Radial distribution of fluoride ion in a cylindrical single crystal of HF-doped ice	29
Figure 43. Radial distribution of chloride ion in a cylindrical single crystal of HCl-doped ice	29
Figure 44. Radial distribution of chloride ion in a cylindrical single crystal of HCl-doped ice	29
Figure 45. Radial distribution of chloride ion in a cylindrical single crystal of HCl-doped ice	29

Tables

1. The concentration of impurity in the ice from given mother solutions	2
2. Values of n determined for pure and doped ice single crystals	4
3. Activation energy of HCl-doped ice crystals	4

Abstract

Constant strain-rate tensile tests were carried out on single crystals of ice doped with various impurities such as HF, HCl, HBr, NH_4OH , NH_4F , NaF, KF, NaOH, H_2O_2 and He. The tests were carried out in the temperature range of -5°C to -53°C . HF-doped crystals showed a softening effect in this temperature range as well as in the lower temperature range previously reported. HCl-doped crystals showed a less pronounced softening effect than HF. H_2O_2 -doped crystals showed a softening effect at -26°C , one He-doped crystal showed a hardening effect at -15°C , and the other impurities had no apparent effect. An activation energy for pure ice of 18 ± 2 kcal/mole was deduced; for HCl-doped ice an activation energy of 12 ± 3 kcal/mole and 13 ± 2 kcal/mole was found using two methods of analysis. A power law relationship between stress and strain-rate was found to hold for pure and HCl-doped crystals with $n = 1.73 \pm 0.07$. The distribution of fluorine and chlorine ions in the crystals showed marked increases in ion concentration towards the surface.

Effect of Impurities on the Mechanical Properties of Ice Single Crystals

T. Nakamura and S. J. Jones

INTRODUCTION

This work was done between 1968 and 1970 when one of the authors (Nakamura) was on leave from the Institute of Snow and Ice Studies, National Research Center for Disaster Prevention, Nagaoka, Japan and held a National Research Council of Canada Post Doctorate Fellowship with the Inland Waters Directorate. This report contains experimental details, all the basic data obtained in the experiments, and the resultant conclusions. Preliminary results have been published (Nakamura and Jones, 1970). In addition, a paper summarizing the conclusions but of necessity omitting much of the data, was presented at a recent conference (Nakamura and Jones, 1973, in press).

The effect of HF, NH₄OH and NH₄F on the mechanical properties of ice single crystals has been reported by Jones and Glen (1969a). These impurities were chosen due to their effect on the electrical properties of ice; they were thought to enter the ice lattice substitutionally (Steinmann, 1957; Gränicher, 1963; Glen, 1969). It was found that at temperatures around -60°C, HF had a softening effect in that the creep rate was greater for HF-doped ice than for pure ice, while NH₄OH had a slight hardening effect and NH₄F had no observable effect. The object of the present work was to investigate the effect of HF, NH₃ and NH₄F at higher temperatures than those used by Jones and Glen (1969a) and to ascertain if any other impurities, which may or may not dissolve substitutionally in ice, had a similar effect.

Ida and others (1966) have reported experiments on the dielectric dispersion of impure ice below -100°C. They found such dispersion only in KOH, NaOH, LiOH, H₂O₂, NH₄F or HF-doped ice, and not in Ba(OH)₂, NH₄OH, HCl or KCl-doped ice. Some of these impurities were chosen to determine if there was a corresponding grouping in terms of mechanical properties.

From dielectric measurements, Young and Salomon (1968) concluded that HCl enters the ice lattice substitutionally, at least at small concentrations. This was another reason for investigating the mechanical properties of HCl-doped ice. The majority of the results reported here are concerned with HCl-doped ice.

While this work was in progress, Kahane and others (1969) showed that the inert gases He and Ne could be dissolved in ice, presumably as an interstitial atom. We have attempted, therefore, to determine the effect helium might

have on ice's mechanical behaviour. Results are given in the temperature range -5°C to -46°C for the following impurities: HF, NH₄OH, NH₄F, HCl, HBr, NaF, KF, NaOH, H₂O₂ and He.

EXPERIMENTAL

Preparation of Crystals

The single crystals were grown in a manner similar to that described previously by Glen & Jones (1967) except that a small immersion heater was inserted in the bowl to prevent the ice from freezing over completely and thus causing a pressure to build up during freezing. A seed crystal was also placed in the water to prevent supercooling which otherwise would sometimes occur. The water used was de-ionized water of greater than 10MΩ-cm resistivity, de-aired by boiling and cooled under vacuum. Except for Helium (the procedure for He is described in the next section), the impurity was added to the water just before growth of the water crystals started. In order to obtain ice crystals with the angle between the tensile and optic axes close to 45°, all glass tubes in the bowl were placed at an angle of 45° to the vertical. After growth of the crystals, the optic axis angle was checked by a polarized light method. Almost all the crystals had c-axis orientations within 6° of 45° to the tensile axis.

Procedure

A crystal was mounted in a metal grip and frozen in place. The grip and crystal were then placed in the upper jaw of an Instron table model mechanical tester, and the crystal frozen into the lower metal grip. All this was done in a cold room at -10°C. A polystyrene box was made to fit around the crystal thus reducing the temperature fluctuations from the cold room. The lowest temperature obtainable using the cold room alone was about -25°C; to obtain lower temperatures, methanol, cooled in a separate cold bath (model Tenney Engineering Inc., MR-9), was passed through coils around the crystal. In this case the temperature was controlled with a platinum resistance thermometer and controller to an accuracy of ±0.05°C. The lowest temperature obtained was -53°C.

All the tests reported here were conducted at a constant velocity of deformation. Since, however, an Instron is a 'hard' machine and since the total strain of a sample was always small - typically less than 5% - this is equivalent to a constant strain-rate.

The concentration of the various ions in the crystals was usually determined by melting the sample after a test and analyzing the water with a pH/mV meter (Orion model 801) and various specific ion electrodes. In the case of NH_4OH and NH_4F , a colorimetric method was used with Nessler's reagent since no specific ion electrode existed for NH_3 . In the case of Helium a different method altogether was used.

The He-doped crystals were prepared by placing a pure ice crystal in a vessel containing Helium gas at a pressure of 125 bars. The crystal was left for at least 24 hours, and then removed and mechanically tested at atmospheric pressure. After the test, the crystal was melted and the amount of Helium gas given off was measured with a microburet system.

RESULTS

General Results

All the crystals used for the tensile tests were good single crystals as determined optically. However, from X-ray topographic studies, it was found that sub-grain boundaries were often present. The sub-grains were typically a few mm in diameter and the boundaries represented misorientations of approximately one minute of an arc. The dislocation density within these sub-grains was at least 10^5 cm^{-2} .

Table 1 shows the concentration of impurities in the mother solution and in the ice crystals formed from the solutions. Relatively large amounts of HF, HCl and NH_4F would enter the ice and it was usually easy to grow single crystals with these impurities. NaF and KF-doped single crystals were very difficult to grow and very little of the impurity was found in the ice. NH_4OH and NaOH-doped crystals were quite easy to grow, but again very little of the impurity had entered the ice. The distribution of the impurity in the ice is discussed in a later section.

The crystals exhibited slip on the basal (0001) plane as shown by one example of slip lines on an NaOH-doped

Table 1. The concentration of impurity in the ice from given mother solutions

Impurity	Concentration of mother solution ppm	Concentration in ice ppm
HF	100	5
HCl	200	2
HBr	60	0.4
NH_4OH	100	0.1
NH_4F	100	10
NaF	20	0.1
KF	~20	0.1
NaOH	100	~0.1
H_2O_2	200	-

crystal in Figure 1. This is the normal mode of deformation in ice, as observed by previous workers (McConnel, 1891; Glen and Perutz, 1954; Higashi *et al.*, 1964; Glen and Jones, 1967).

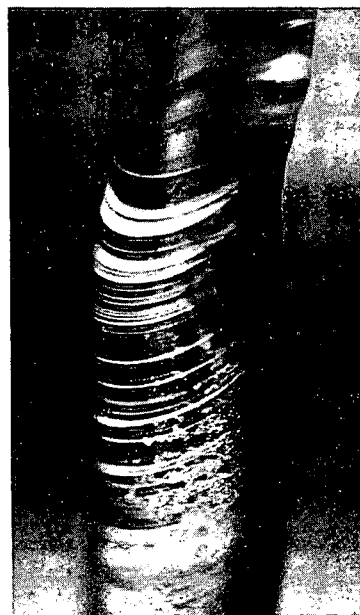


Figure 1. Basal Slip lines on an NaOH-doped single crystal of ice deformed 20% at -26°C .

Resolved shear stresses and resolved shear strains used in this work are defined by Schmid & Boas (1968, p. 60).

Unfortunately, the results obtained from a number of nominally pure crystals all tested at the same strain-rate and temperature were not entirely reproducible, as will be seen when studying the various figures. For example, Figure 8 shows results from three pure crystals tested at a strain-rate of $1.6 \times 10^{-6} \text{ s}^{-1}$ at -26°C . As can be seen, the curves vary in stress by a factor of 1.3. It is believed that this variation is due to differences in the initial number of dislocations present in the crystal.

HF-doped Crystals

Figure 2 shows typical stress-strain curves for pure and HF-doped crystals at -11°C for a number of different strain-rates as marked on the figure. The curves show an initial increase in stress up to a maximum or 'yield' stress followed by a continuous decrease in stress, as found by previous workers. No work hardening was observed. Figure 2 shows that the HF-doped crystals were somewhat softer than pure ice in that the stress level required to maintain the constant strain-rate was lower for the HF-doped crystals. This is particularly true of the maximum stress reached. If one plots the maximum resolved shear stress against the resolved strain-rate, one obtains such curves as are shown for -11°C in Figure 3. Figure 3 shows that, for a given stress, the strain-rate of

the HF-doped ice is 6 times that of the pure ice. Similar results at -30°C (Fig. 4-7) indicate an increase in strain-rate of a factor of 7. Some additional results at -26°C are shown in Figure 8. There is a suggestion in Figures 3 and 7 that the effect of the HF is smaller at higher strain-rates but this may be an artifact due to the greater amount of data collected at the higher strain-rates. As has been mentioned there is some scatter in the data but as far as could be detected there was no systematic dependence on the amount of impurity.

HCl-doped Crystals

Preliminary results for HCl-doped ice have been published (Nakamura and Jones, 1970). Figures 9-12 show the stress-strain curves obtained at -26°C for pure and HCl-doped ice at various strain-rates and Figure 13 shows the maximum shear stress plotted as a function of strain-rate. Least squares straight lines have been fitted to the pure data and the HCl-doped data on Figure 13. The HCl-doped crystals have a strain-rate that is about a factor of 3 greater than the pure ice. Figures 14 and 15 show the data collected at -46°C ; Figures 16, 17 and 18 show the data collected at -15°C and Figures 19, 20 and 21 show the data collected at -5.6°C . Figure 18 contains also two points which refer to He-doped ice; these will be discussed in the He section on doped crystals. Comparing Figures 13, 15, 18 and 21 there seems to be a significant softening at -46°C and -26°C but very little, if any, at -15°C and -5.6°C . This suggests that the activation energy of the HCl-doped ice is less than that for pure ice. A direct determination of this activation energy also gives a value (12 ± 3 kcal/mole) less than for pure ice (18 ± 2 kcal/mole) as shown in the section headed "Activation Energy of Pure and HCl-doped Crystals".

H₂O₂-doped Crystals

Results for 2 crystals of H₂O₂-doped ice are shown in Figure 22, for a temperature of -26°C . Although the data is limited there appears to be a softening effect since the stress level for the doped ice is about a factor of three less than for the pure crystals.

NH₄OH-doped Crystals

Jones and Glen (1969a) showed that ammonium-doped ice crystals had a slight hardening effect at about -60°C . This effect was examined at higher temperatures and the results at -11°C are shown in Figures 23 and 24. A slight softening is apparent although there is some scatter in the data. At -26°C there was no effect of the NH₄OH (Figure 25).

HBr-doped Crystals

While it was not expected that HBr would enter the ice lattice substitutionally because of the radius of the Br atom (1.96 Å) as compared to that of the oxygen atom (1.38 Å), two specimens were tested at -26°C and it was observed that there was no significant difference between these crystals and pure ice (see Fig. 26).

NH₄F-doped Crystals

Only two crystals were tested, one at -11°C and one at -26°C , and in both cases there was no significant difference from pure ice. This is in agreement with the data of Jones and Glen (1969a) at lower temperatures.

NaF-doped Crystals

Three crystals were tested at -26°C and no significant effect of the NaF was observed (Fig. 27).

KF-doped Crystals

Only one crystal was tested at -33°C as shown in Figure 28, and no effect was observed.

NaOH-doped Crystals

Five crystals were tested at -26°C and the results are shown in Figure 29. No difference was observed between these and pure crystals (Fig. 30) but only small amounts of NaOH entered the ice samples (≤ 0.1 ppm) and at this level our method of determining the concentration was not reliable.

He-doped Crystals

The results from only two crystals are shown in Figure 31 and the maximum stress values are plotted on Figure 18. Apparently the crystal containing ≈ 400 ppm. Helium was harder than pure ice, but a second crystal prepared in the same manner contained zero Helium when it was analyzed. This was because the Helium was diffusing out of the specimen in a shorter time than it took to do the mechanical test. The diffusion coefficient of Helium in ice has recently been measured by two groups of workers. Davy and Miller (1970) have reported a value of $10^{-6} \text{ cm}^2 \text{ s}^{-1}$ at -10°C , and Haas and others (1971) give $D \approx 10^{-5}$ at -10°C with a strong anisotropy.

Dependence of Strain-rate on Stress

Previous workers (Higashi, 1969; Readey & Kingery, 1964; Jones and Glen, 1969b) have found that for pure ice the strain-rate, $\dot{\epsilon}$ can be expressed as a function of stress, τ , as $\dot{\epsilon} \propto \tau^n$ where n is a constant or a function of stress (Jones and Glen, 1969b).

There are two ways in which this relationship can be investigated; different samples can be tested at different strain-rates and the stresses recorded, or one sample can be stressed at different strain-rates. The first method leads to such curves as Figure 3 etc. from which n can be determined from the slope of the lines. The second method avoids the lack of reproducibility due to different crystals; with this method a crystal is strained at one strain-rate and then the strain-rate is changed to a higher (or lower) value. The two values of stress, immediately before and after the change in strain-rate, are noted and then a curve of stress against strain-rate is plotted. Such a

curve is shown in Figure 32 and from the slope of the straight lines the value of n is determined. Table 2 summarizes all the n values we have obtained using both methods of determination for various pure and doped samples. A mean $n = 1.73 \pm 0.07$ is obtained for all the crystals.

Table 2. Values of n determined for pure and doped ice single crystals

Crystal	Temperature °C	n	Mean n
Pure	-16	1.7	1.73 ± 0.07
	-12	1.8	
	-6	1.6	
	-11	1.5	
	-15	1.7	
	-26	1.4	
	-30	2.0	
	-46	2.5	
HCl	-6	1.9	
	-53	1.6	
	-26	1.6	
	-6	1.7	
	-15	1.6	
	-26	1.4	
	-11	1.4	
-46	1.8		
NH ₄ OH	-5	2.2	
NH ₄ F	-9	1.7	
NaOH	-26	1.4	
HF	-30	1.3	

Activation Energy of Pure and HCl-doped Crystals

It is generally accepted that the dependence of creep deformation on temperature is given by an Arrhenius equation:

$$\dot{\epsilon} \propto \tau^n \exp(-Q/RT) \quad (2)$$

where $\dot{\epsilon}$ is strain-rate, τ is stress, n is a constant, Q is an activation energy, (strictly an activation enthalpy) R is the gas constant and T is the absolute temperature. This equation can be re-written as:

$$\tau \propto \dot{\epsilon}^{1/n} \exp(+Q/nRT) \quad (3)$$

so that for a constant strain-rate the dependence of τ on T will give Q/n , (Higashi, 1969). If n is known from other tests as in the section "Dependence of Strain-rate on Stress" then Q can be determined. We attempted to measure Q in this way for HCl-doped ice. The tests were done by taking one specimen and straining it at a constant rate and temperature, and then changing the temperature and observing the new stress required to maintain the same strain-rate. The results are shown in

Figures 33 to 36. The time between the end of one test and the beginning of the new one at the new temperature varied from 1-10 hours. The stress immediately before the temperature change is compared with the stress immediately afterwards and these results are shown plotted against $1/T$ in Figure 37. Using the value of 1.73 for n given in the previous section, values of Q were obtained (see Table 3). There is quite a scatter in the results but a mean activation energy is 12 ± 3 kcal/mole for HCl-doped ice.

A second method, which avoided the need to know n , was also used to determine the activation energy of both pure and HCl-doped ice. From the data given in Figs. 1-21 the strain-rate required to give a certain maximum resolved shear stress at different temperatures was determined and plotted as shown in Figures 38 and 39. Figure 38 shows data for HCl-doped ice at three different stresses and Figure 39 shows data for pure ice at two different stresses. The slope of the lines is proportional to the activation energy and is found to be 13 ± 2 kcal mole⁻¹ for HCl-doped ice and 18 ± 2 kcal mole⁻¹ for pure ice. The two values of activation energy for HCl-doped ice obtained by different methods are in good agreement. The value for pure ice of 18 kcal mole⁻¹ is based on less data than the HCl-doped result and is rather high compared to previous workers. Nevertheless, using these two values of activation energy we have reduced all our stress/strain-rate data for pure and HCl-doped ice to one temperature, -26°C. This temperature was chosen because a lot of our data was obtained at that temperature. Pure ice data was reduced using an activation energy of 18 kcal mole⁻¹ and HCl-doped ice data was reduced using an activation energy of 13 kcal mole⁻¹. The result is shown in Figure 40. The line drawn on the graph indicates a demarcation between the pure and HCl data. To the left of the line lie 92% of the HCl-doped data points and to the right of the line 75% of the pure points. This shows a softening effect of HCl despite the scatter in the data.

Distribution of Ions in Single Crystals

The distribution of HF and HCl ions in the doped crystals was examined. A doped crystal was allowed to melt in successive stages and two or three water samples were collected. Figures 41 and 42 show HF results while

Table 3. Activation energy of HCl-doped ice crystals

Sample	Concentration HCl ppm	Mean activation energy of sample kcal. mole ⁻¹
HCl-A	2.0	8.9
HCl-C	2.0	8.7
HCl-D ₁	2.5	12.5
HCl-D ₂	2.5	16.6

Mean activation energy = 12 ± 3 kcal. mole⁻¹.

Figures 43-45 give the HCl results. All show higher ion concentration at the surface than at the centre of the specimen. There were two variations of the experiment, wiping a thin layer off the crystal with a tissue (Figs. 41, 43, 45) or not wiping as the case may be (Figs. 42, 44). For the tensile tests the specimens were wiped with a tissue before testing and so the distribution of the ions in the specimen presumably corresponded to Figures 42, 44. As can be seen from these figures the distribution of HF was much more uniform than of HCl — reflecting the higher diffusion coefficient of HF (Krishnan and Salomon, 1969; Kopp and others, 1965; Haltenorth and Klinger 1969). The reason for such a concentration curve is thought to be that as the ice grows the ions are rejected to the melt preferentially at the centre of the crystal, but become trapped at the ice-glass interface.

CONCLUSIONS AND DISCUSSION

HF had a softening effect at high temperatures (-11°C) as well as low temperatures (-70°C); HCl had a smaller softening effect; HBr, NH_4F , NaF, KF, NaOH had no observable effect; NH_4OH showed a possible slight softening; H_2O_2 showed a softening effect. One Helium specimen showed a hardening effect.

The HF result was similar to that observed by Jones and Glen (1969a) and therefore can be explained by the same theory developed by Glen (1968) concerning the interaction of dislocations and point defects in ice. He has pointed out that due to the random positions of the hydrogen atoms in the ice lattice, a moving dislocation would create point defects of either the ionic or Bjerrum sort (Bjerrum 1951, 1952); he has calculated that this would require a stress of 4300 bar, a value far in excess of the stress needed (about 1 bar) to deform ice plastically. From this theory the result is a dislocation line held up at a number of points along its length until such time as one of the naturally occurring point defects passes and reorients the bond, thus allowing the dislocation line to move forward. When HF is dissolved in ice it is thought to enter the lattice substitutionally and by doing so it introduces Bjerrum and ionic defects (Gränicher 1963; Glen 1969). Kröger (1964) has shown that the number of L type Bjerrum defects increases with rising HF content and in the limit of high concentrations becomes equal to the HF concentration. Since the number of point defects has been greatly increased by the HF, the probability of reorientation of a bond which is holding up a dislocation is greatly increased. The dislocation will move faster and so the ice will be softer. Recently Jones and Gilra (1972) have shown that the diffusion of HF into ice causes a marked increase in dislocation density, which can account for the mechanical softness of HF-doped ice. This may be a result of dislocation multiplication brought about by the increased number of point defects introduced by the HF. If HCl goes into the ice lattice substitutionally as suggested by Young and Salomon (1968) and more recently by Seidensticker (1972), then it will presumably behave like HF and hence the softening effect of HCl can be explained in the same

way as HF. There is no evidence that HBr, NaF or KF enter the ice lattice substitutionally, although it might be expected that the F^- ion could enter the lattice as it does with HF. The fact that we observed no effect of NaF or KF suggests that the F^- ion does not in fact substitute for the O atom in these cases. Kelly and Salomon (1969) believe from dielectric measurements of polycrystalline ice that NaOH does not enter the lattice substitutionally either. The slight softening of NH_4OH doped specimens at -11°C is in apparent contradiction to Jones and Glen (1969a) who observed a hardening effect at -60°C . Our results, however, show a large scatter, and so perhaps it is not reasonable to propose a theory to explain this contradiction until the experimental evidence is clear. Nevertheless this apparent contradiction could be explained by postulating that the many D defects introduced by the NH_3 are mobile at the high temperature but immobile at the lower temperature. This implies that NH_4OH -doped ice would have a higher activation energy for creep than pure ice.

Foley and Giguère (1951) studied the phase equilibrium of the system H_2O_2 - H_2O and concluded that solid solutions are not formed. We had no means of testing for the presence of H_2O_2 in our samples but from comparison with other impurities we would expect there to be only a few ppm present. Foley & Giguère (1951) would not have detected such small quantities in their experiment. If H_2O_2 can enter the ice substitutionally in these small quantities it might introduce L-defects and so behave like HF. This would then account for the apparent softening.

Helium, being an inert gas, must enter the ice lattice as an interstitial atom. As such, it could act as a pinning point for dislocation and hence slow them down. This would give an apparent hardening.

Our value of $n = 1.73$ is close to the value, in the same temperature range, observed by previous workers. Higashi and others (1964) found $n = 1.53$ in tensile, constant strain-rate tests and 1.58 in bending creep tests (Higashi and others, 1965). Readey and Kingery (1964) obtained $n = 2.0$ and Muguruma (1969) found $n = 1.3$ and $n = 1.7$ for chemically polished and mechanically polished specimens respectively. Jones and Glen (1969b) found $n = 2.3$ at -70°C indicating that n increases with decreasing temperature.

The value of activation energy for pure ice obtained in this work, 18 ± 2 kcal/mole, is somewhat higher than that obtained by previous workers: Higashi and others (1964) obtained 15.8 kcal/mole in bending creep experiments, Readey and Kingery (1964) obtained 14.3 kcal/mole, Jones and Glen (1969) obtained 15.6 kcal/mole in tensile creep experiments above -50°C and 9.6 ± 0.5 kcal/mole below -50°C . Our value for HCl-doped ice is about 3 kcal/mole less than that obtained for pure ice by these workers.

ACKNOWLEDGMENTS

We are grateful to G.A. Barnett for technical assistance in the laboratory.

REFERENCES

- Bjerrum, N., 1951. Structure and properties of ice. *K. danske Vidensk. Selsk. Mat.-fir. Medd.*, Vol. 27, p. 3-56.
- Bjerrum, N., 1952. Structure and properties of ice. *Science*, Vol. 115: 385-390.
- Davy, J.G., and K.W. Miller. 1970. The diffusion of helium through ice. *Solid State Communications*, Vol. 8:1459-61.
- Foley, W.T., and P.A. Giguère. 1951. Hydrogen peroxide and its analogues. II Phase equilibrium in the system hydrogen peroxide - water. *Canadian Journal of Chemistry*, Vol. 29: 123-32.
- Glen, J.W., and M.F. Perutz. 1954. Growth and deformation of ice crystals. *Journal of Glaciology*, Vol. 2:397-412.
- Glen, J.W., and S.J. Jones. 1967. The deformation of ice single crystals at low temperatures. (Oura, H., ed. *Physics of snow and ice; international conference on low temperature science*. 1966 Proceedings, Vol. 1, Pt. 1, [Sapporo], Institute of Low Temperature Science, Hokkaido University, p. 267-75.
- Glen, J.W. 1968. The effect of hydrogen disorder on dislocation movement and plastic deformation of ice. *Physik der kondensierten Materie*, Vol. 7:43-51.
- Glen, J.W. 1969. Structure and point defects in ice: their effect on the electrical and mechanical properties. *Science Progress, Oxford*, Vol. 57:1-21.
- Gränicher, H. 1963. Properties and lattice imperfections of ice crystals and the behaviour of H₂O - HF solid solutions. *Physik der kondensierten Materie*, Vol. 1:1-12.
- Haas, J., B. Bullemer and A. Kahane. 1971. Diffusion de l'Helium dans la glace monocristalline. *Solid State Communications*, Vol. 9:2033-35.
- Haltenorth, H., and J. Klinger. 1969. Diffusion of hydrogen fluoride in ice. In *Physics of ice: Proceedings of the international symposium on physics of ice, Munich, Germany, September 9-14, 1968*. Edited by N. Riehl, B. Bullemer, H. Engelhardt, New York, Plenum Press, p. 579-84.
- Higashi, A., S. Koinuma and S. Mae. 1964. Plastic yielding in ice single crystals. *Japanese Journal of Applied Physics*, Vol. 3: 610-16.
- Higashi, A., S. Koinuma and S. Mae. 1965. Bending creep of ice single crystals. *Japanese Journal of Applied Physics*, Vol. 4: 578-82.
- Higashi, A. 1969. Mechanical properties of ice single crystals. *Physics of ice: Proceedings of the international symposium on physics of ice, Munich, Germany, September 9-14, 1968*. Edited by N. Riehl, B. Bullemer, H. Engelhardt, New York, Plenum Press, p. 197-212.
- Ida, M., N. Nakatani, K. Imai, and S. Kawada. 1966. Dielectric dispersion of impure ice at low temperatures. *Science Reports of Kanazawa University*, Vol. 11:13-22.
- Jones, S.J. and N.K. Gilra. 1972. Increase of dislocation density in ice by dissolved hydrogen fluoride. *Applied Physics Letters*, Vol. 20:319-20.
- Jones, S.J. and J.W. Glen. 1969a. The effect of dissolved impurities on the mechanical properties of ice crystals. *Philosophical Magazine*, Vol. 19:13-24.
- Jones, S.J. and J.W. Glen. 1969b. The mechanical properties of single crystals of pure ice. *Journal of Glaciology*, Vol. 8:463-73.
- Kahane, A., J. Kinger and M. Philippe. 1969. Dopage selectif de la glace monocristalline avec de l'helium et du néon. *Solid State Communications*, Vol. 7:1055-56.
- Kelly, D.J. and R.E. Salomon. 1969. Dielectric behaviour of NaOH-doped ice. *Journal of Chemical Physics*, Vol. 50:75-79.
- Kopp, M., D.E. Barnaal, and I.J. Lowe. 1965. Measurement by N.M.R. of the diffusion rate of HF in ice. *Journal of Chemical Physics*, Vol. 43:2965-71.
- Krishnan, P.N. and R.E. Salomon. 1969. The solubility of hydrogen chloride in ice. *Journal of Physical Chemistry*, Vol. 73:2680-83.
- Kröger, F.A. 1964. *The chemistry of imperfect crystals*. (Amsterdam: North Holland) p. 750.
- McConnel, J.C. 1891. On the plasticity of an ice crystal. *Proceedings of Royal Society (London)*, Vol. 49:323-43.
- Muguruma, J. 1969. Effects of surface conditions on the mechanical properties of ice crystals. *British Journal of Applied Physics (Journal of Physics D)*, Ser. 2, Vol. 2:1517-25.
- Nakamura, T. and S.J. Jones. 1970. Softening effect of dissolved hydrogen chloride in ice crystals. *Scripta Metallurgica*, Vol. 4, No. 2:123-26.
- Nakamura, T. and S.J. Jones. 1973. Mechanical properties of impure ice crystals. *Physics and Chemistry of Ice*. Edited by E. Whalley, S.J. Jones and L.W. Gold. Royal Society of Canada (in press).
- Readey, D.W. and W.D. Kingery. 1964. Plastic deformation of single crystal ice. *Acta Metallurgica*, Vol. 12:171-78.
- Schmid, E. and W. Boas. 1968. *Plasticity of crystals with special reference to metals*. Chapman and Hall, London. (Re-issue of 1950 edition by F.A. Hughes & Co. Ltd.)
- Seidensticker, R.G. 1972. Partitioning of HCl in the water-ice system. *Journal of Chemical Physics*, Vol. 56:2853-57.
- Steinemann, A. 1957. Dielektrische eigenschaften von Eiskristallen. II teil dielektrische Untersuchungen an Eiskristallen mit eingelagerten Fremdatomen. *Helvetica Physica Acta*, Vol. 30:581-610.
- Young, I.G. and R.E. Salomon. 1968. Dielectric behaviour of ice with HCl impurity. *Journal of Chemical Physics*, Vol. 48:1635-44.

Appendix

(Figures 2 to 45)

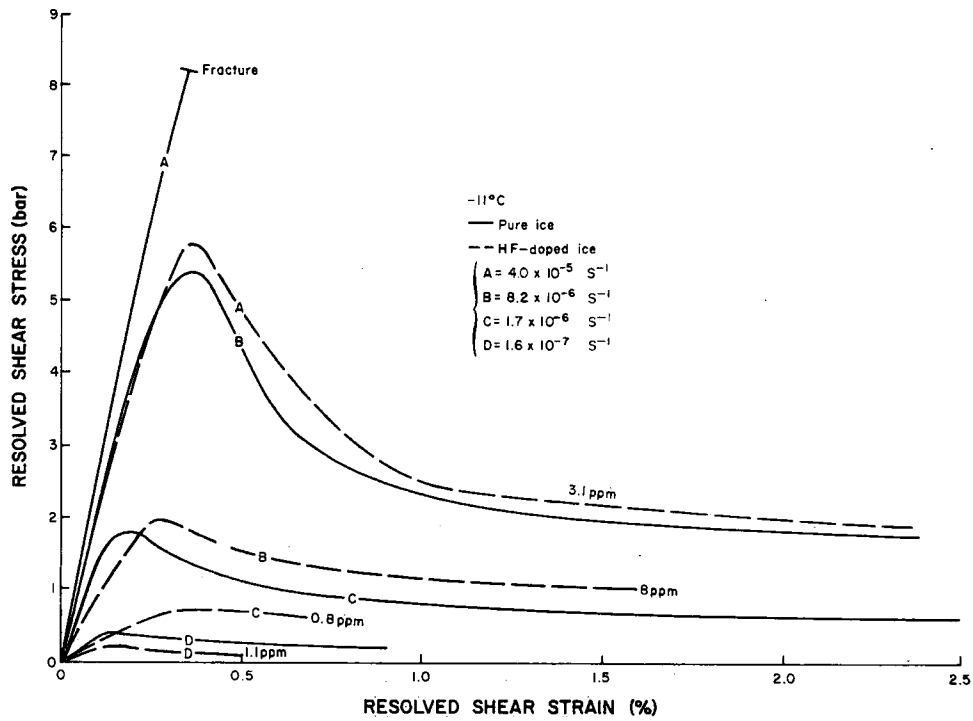


Figure 2. Stress-strain curves for pure and HF-doped ice deformed at -11°C and various strain-rates and dopant concentrations as marked on the figure.

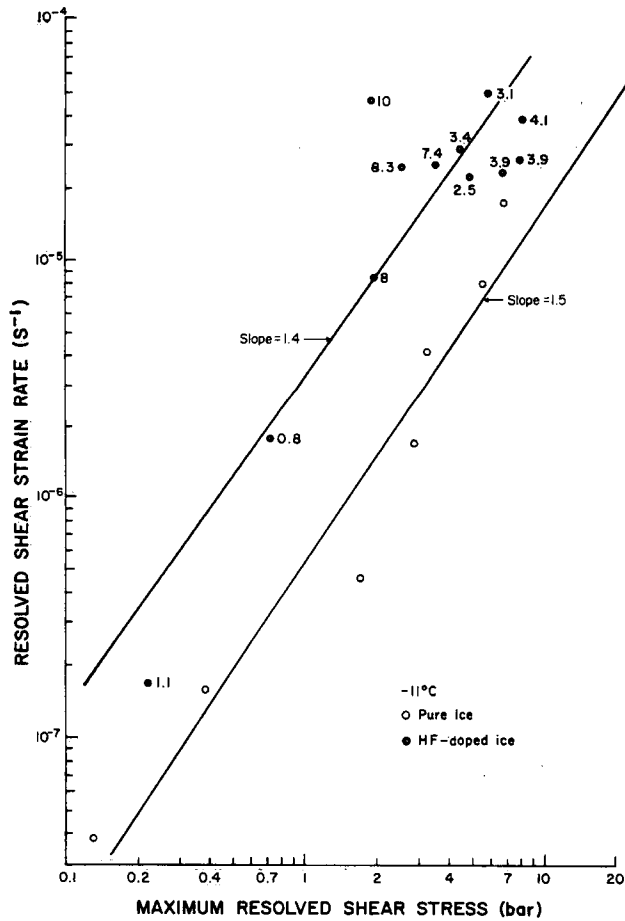


Figure 3. Maximum resolved shear stress plotted against strain-rate for pure and HF-doped ice at -11°C . The number beside each filled circle is the HF concentration, in ppm, of the sample.

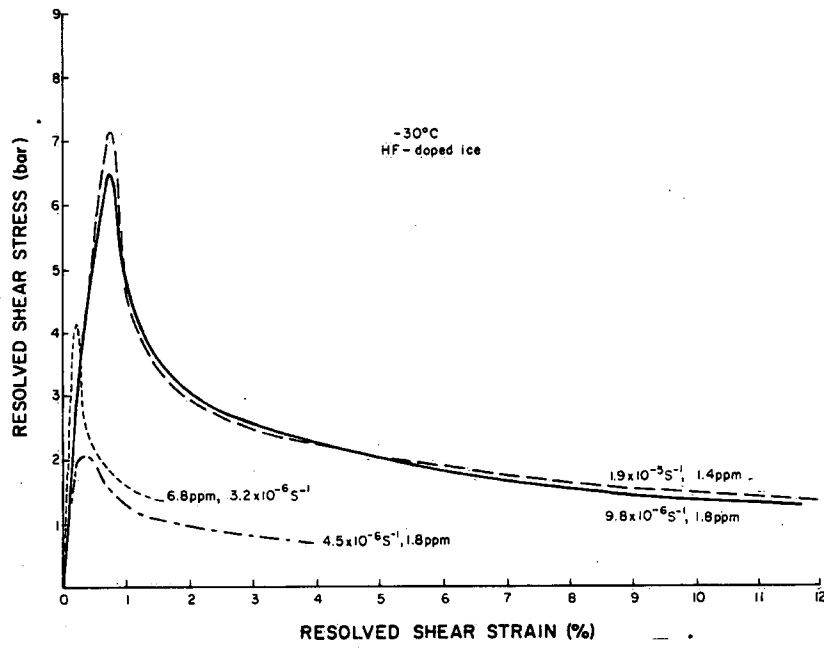


Figure 4. Stress-strain curves for HF-doped ice deformed at -30°C and various strain-rates as marked on the figure.

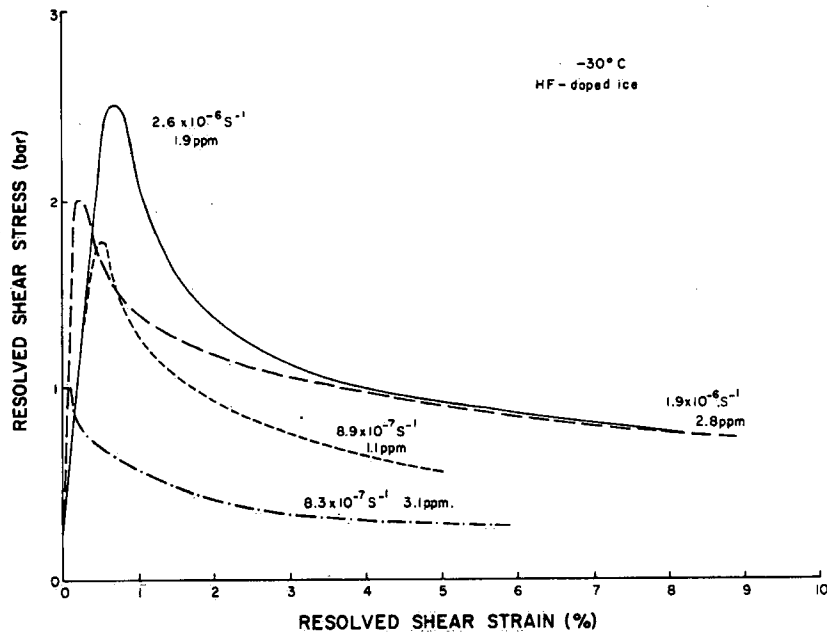


Figure 5. Stress-strain curves for HF-doped ice deformed at -30°C and various strain-rates as marked on the figure.

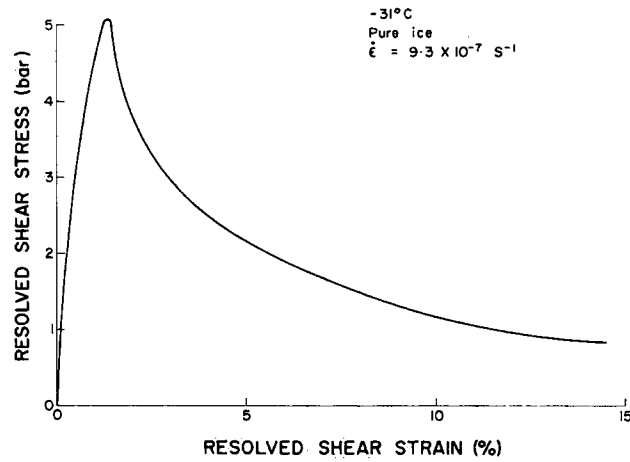


Figure 6. Stress-strain curve of one pure ice crystal deformed at -31°C at a strain-rate of $9.3 \times 10^{-7} \text{ s}^{-1}$.

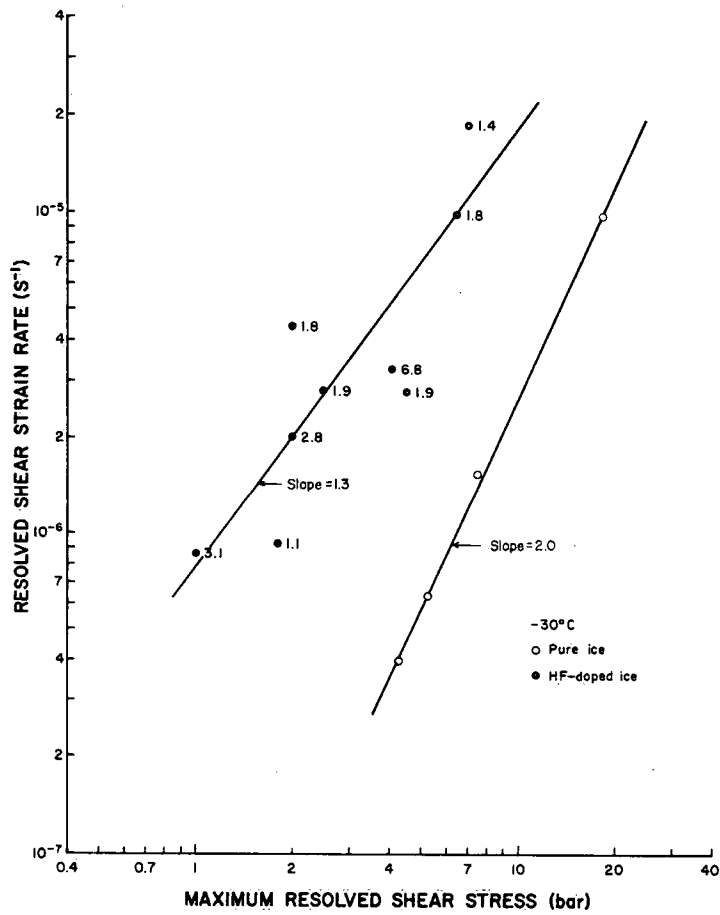


Figure 7. Maximum resolved shear stress plotted against strain-rate for pure and HF-doped ice deformed at -30°C . The number beside each filled circle is the HF concentration of the sample, in ppm.

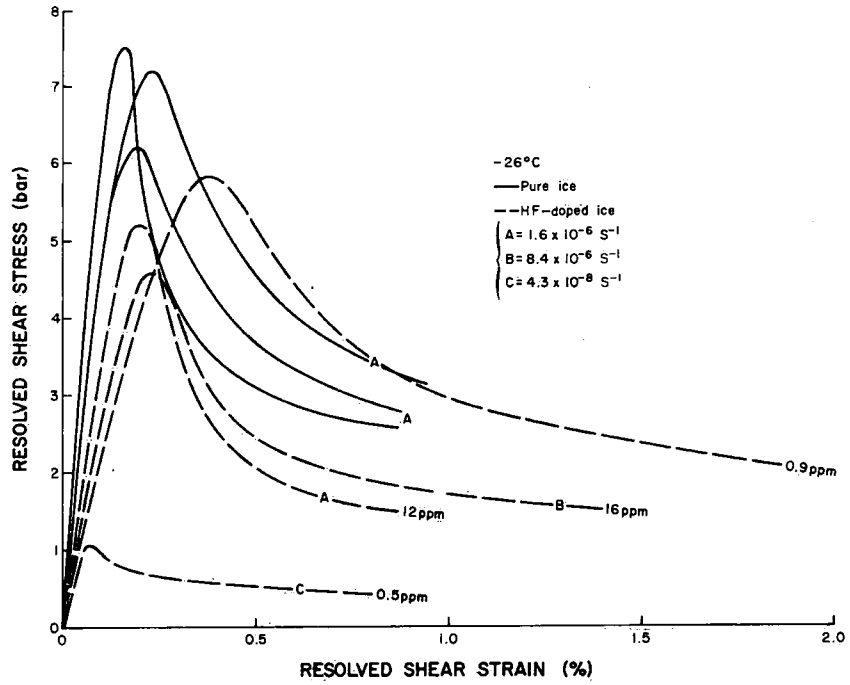


Figure 8. Stress-strain curves for pure and HF-doped ice deformed at -26°C and various strain-rates and dopant concentrations as marked on the figure.

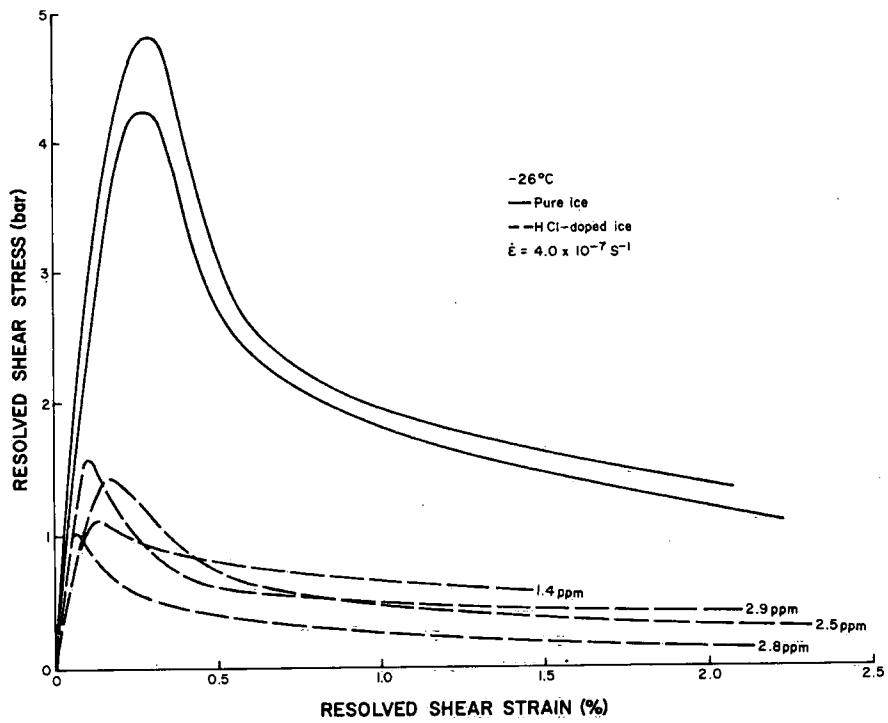


Figure 9. Stress-strain curves for pure and HCl-doped ice deformed at -26°C at a strain-rate of $4 \times 10^{-7} \text{ s}^{-1}$.

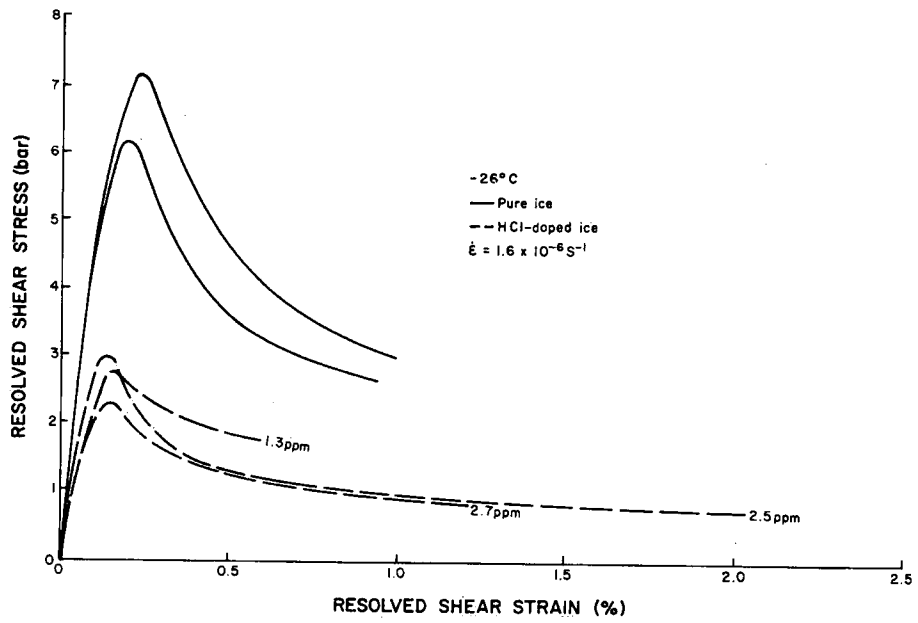


Figure 10. Stress-strain curves for pure and HCl-doped ice deformed at -26°C at a strain-rate of $1.6 \times 10^{-6} \text{ s}^{-1}$.

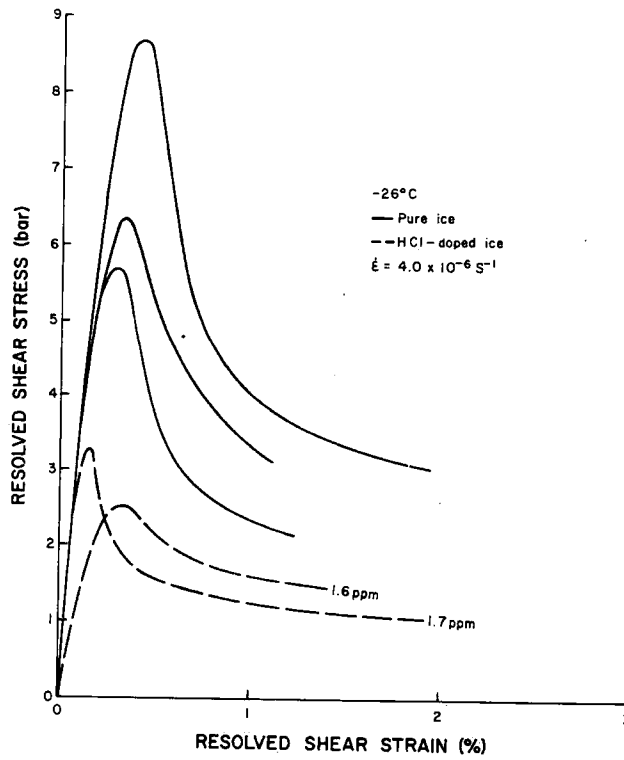


Figure 11. Stress-strain curves for pure and HCl-doped ice deformed at -26°C at a strain-rate of $4 \times 10^{-6} \text{ s}^{-1}$.

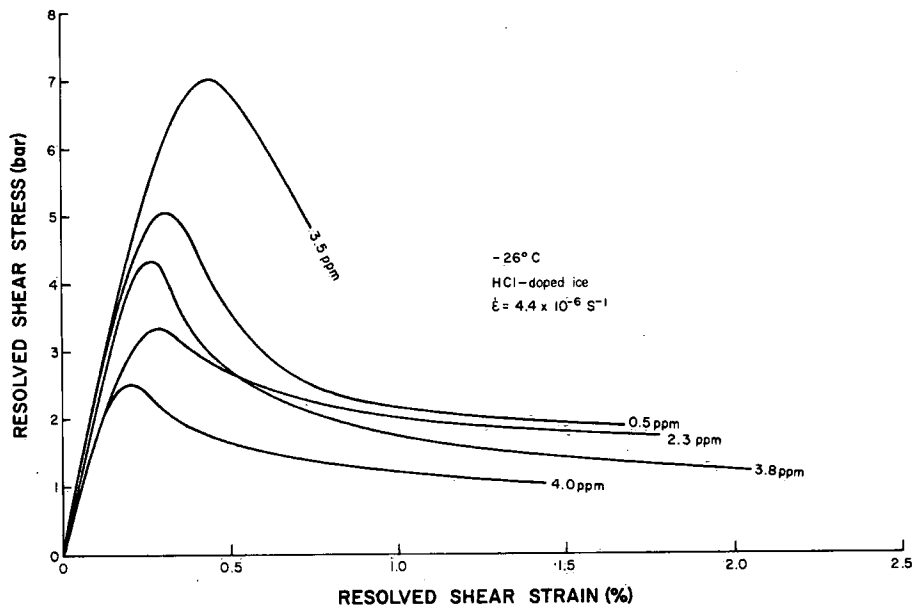


Figure 12. Stress-strain curve for HCl-doped ice deformed at -26°C at a strain-rate of $4.4 \times 10^{-6} \text{ s}^{-1}$.

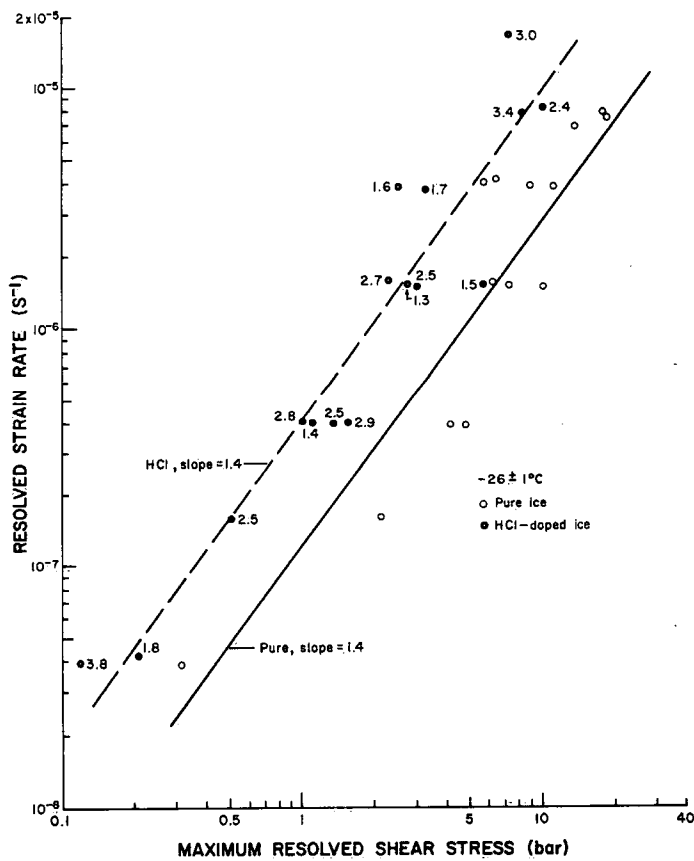


Figure 13. Maximum resolved shear stress plotted against strain-rate for pure and HCl-doped ice deformed at -26°C . The number beside each filled circle is the HCl concentration of the sample in ppm.

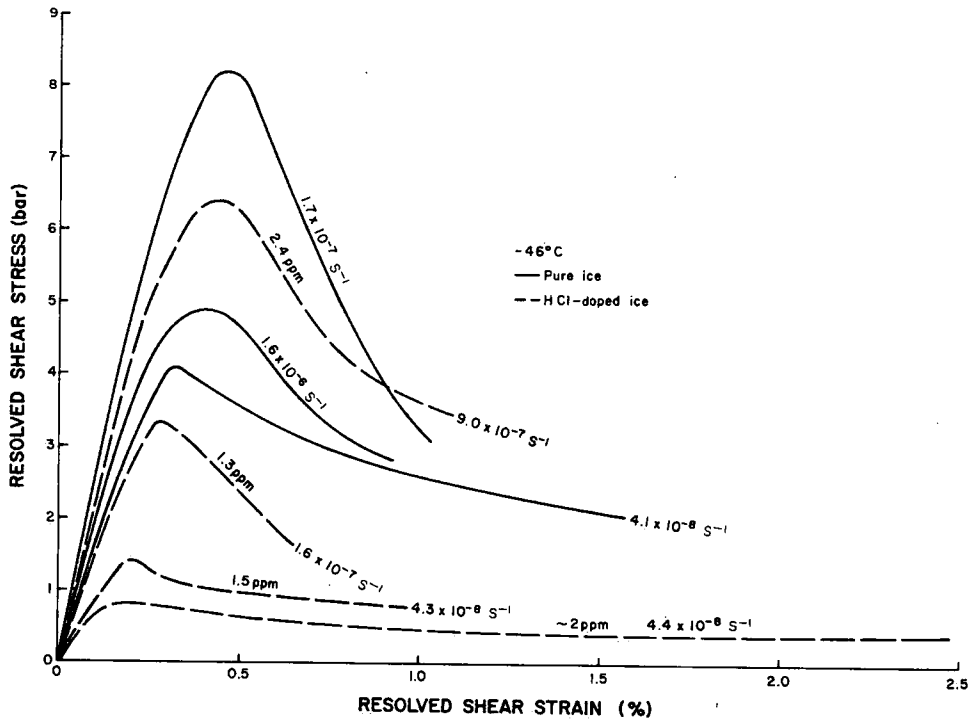


Figure 14. Stress-strain curves of pure and HCl-doped ice deformed at -46°C at various strain-rates as marked on the figure.

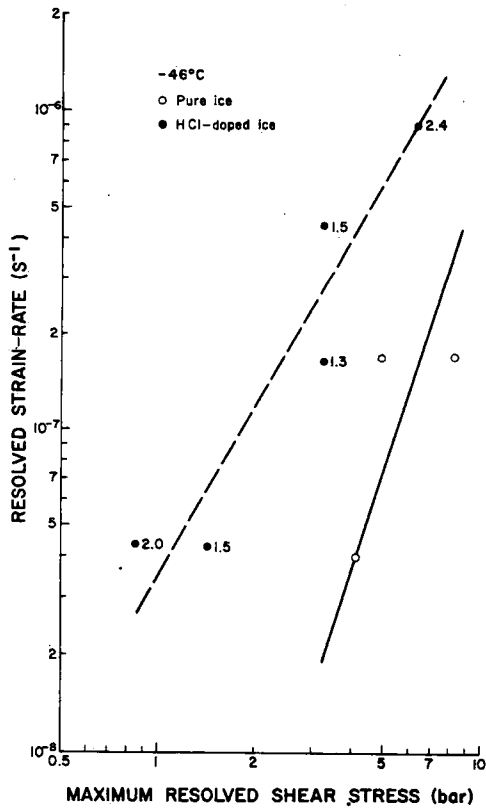


Figure 15. Maximum resolved shear stress plotted against strain-rate for pure and HCl-doped ice deformed at -46°C . The number beside each filled circle is the HCl concentration of the sample, in ppm.

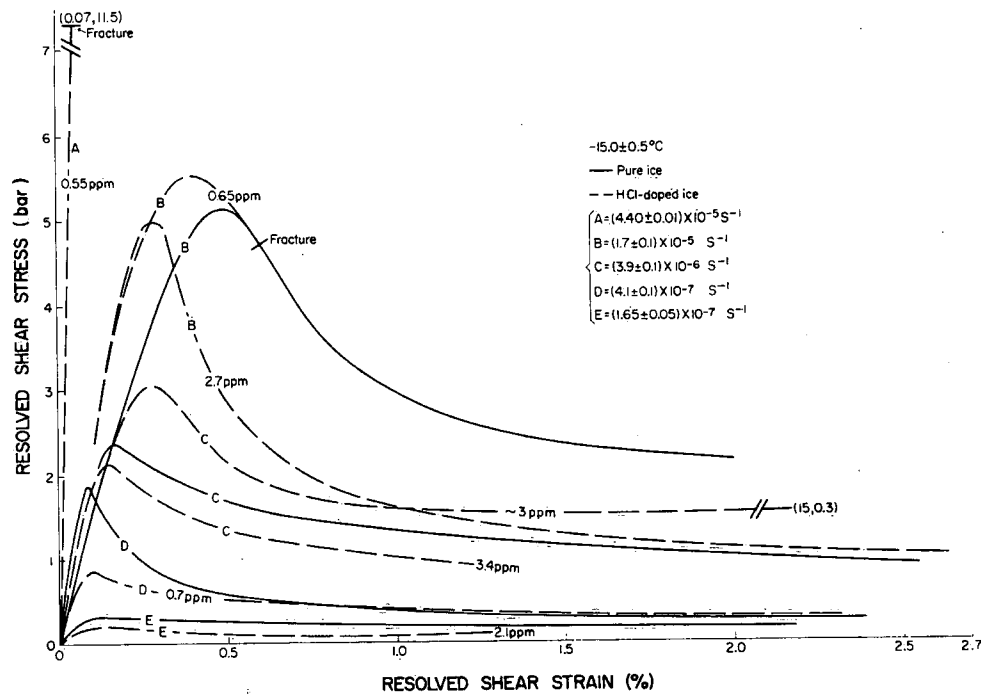


Figure 16. Stress-strain curves for pure and HCl-doped ice deformed at -15°C at various strain-rates and dopant concentrations as marked on the figure.

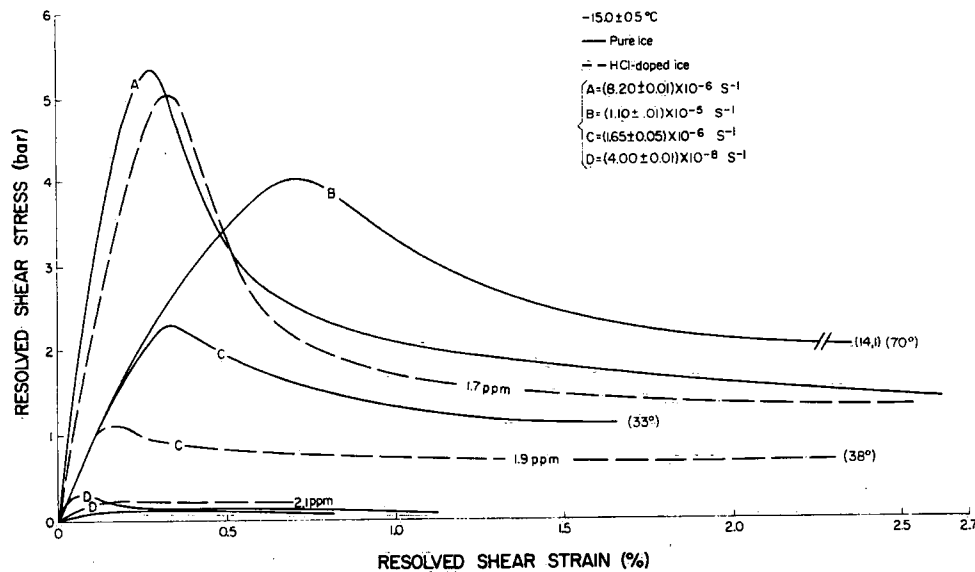


Figure 17. Stress-strain curves for pure and HCl-doped ice deformed at -15°C at various strain-rates as marked on the figure.

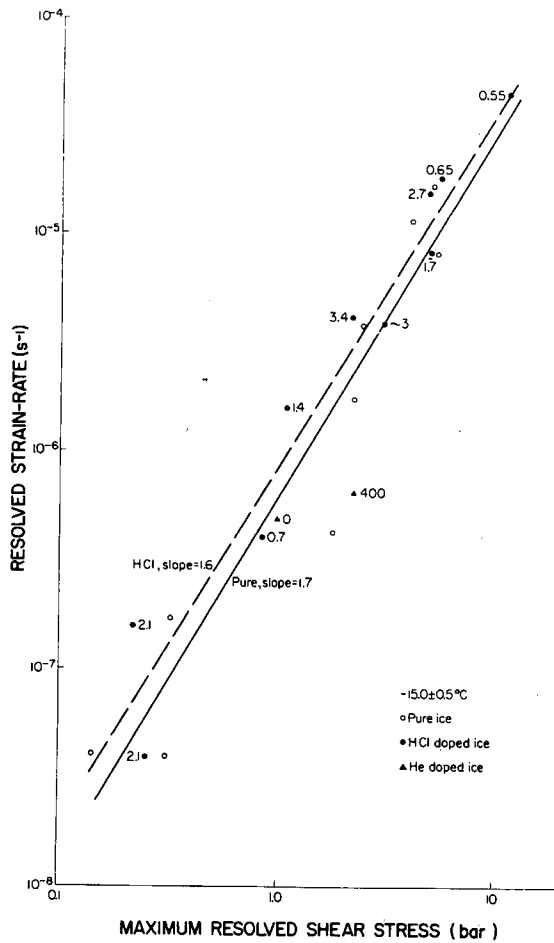


Figure 18. Maximum resolved shear stress plotted against strain-rate for pure, HCl-doped and He-doped ice at $-15^\circ C$. The dopant concentration is marked for each sample.

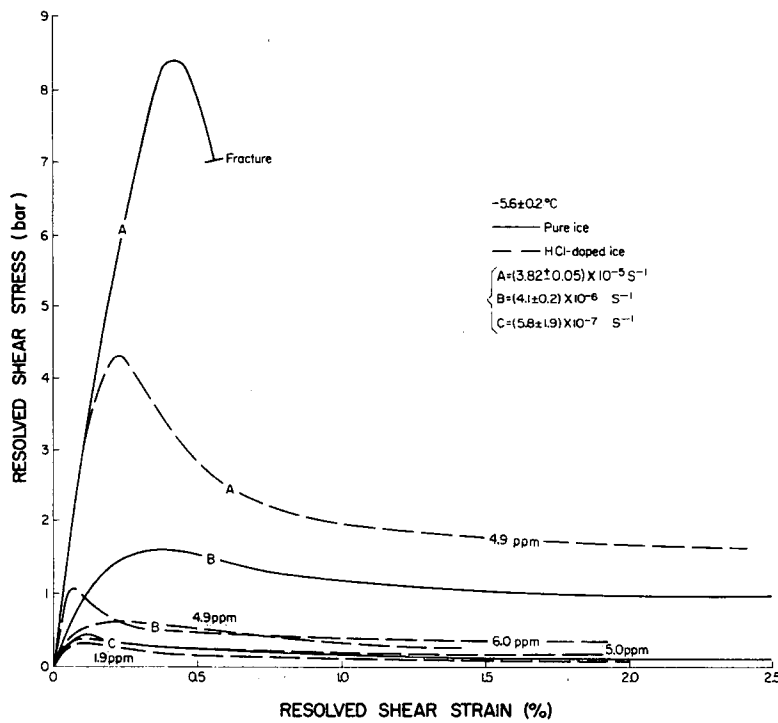


Figure 19. Stress-strain curves for pure and HCl-doped ice deformed at $-5.6^\circ C$ at various strain-rates as marked.

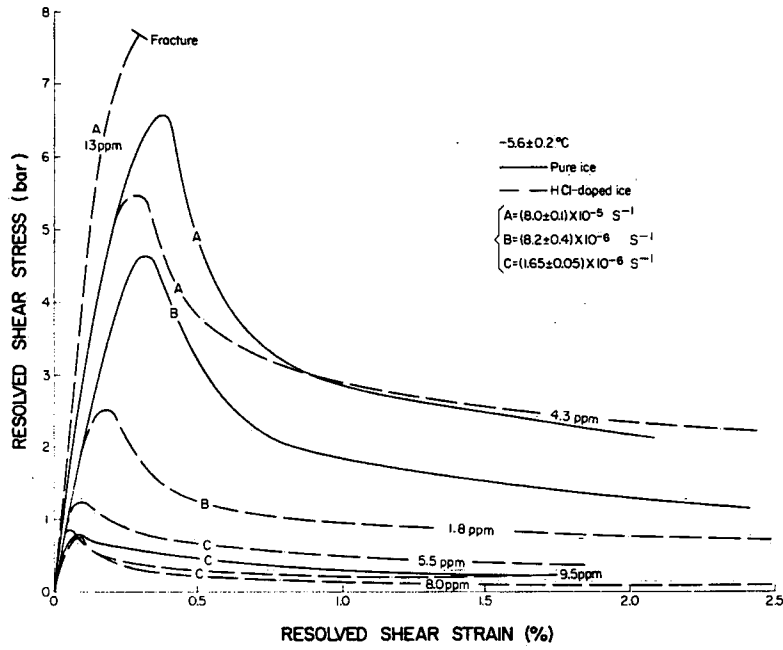


Figure 20. Stress-strain curves for pure and HCl-doped ice deformed at -5.6°C at various strain-rates as marked.

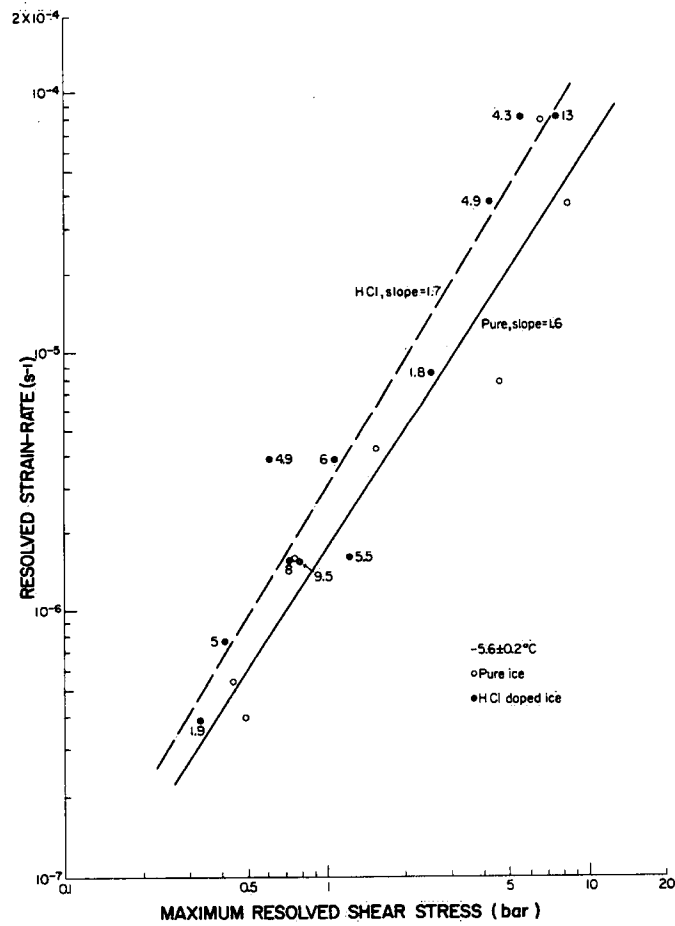


Figure 21. Maximum resolved shear stress plotted against strain-rate for pure and HCl-doped ice at -5.6°C . The number beside each filled circle is the HCl concentration in the sample, in ppm.

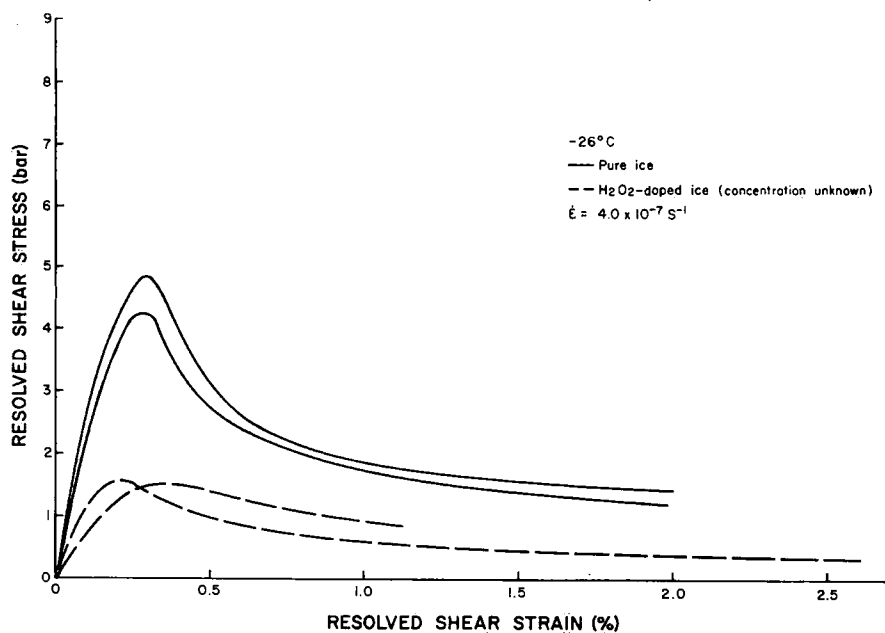


Figure 22. Stress-strain curves for two H₂O₂-doped samples and two pure ice samples deformed at -26°C at a strain-rate of $4 \times 10^{-7} \text{ s}^{-1}$.

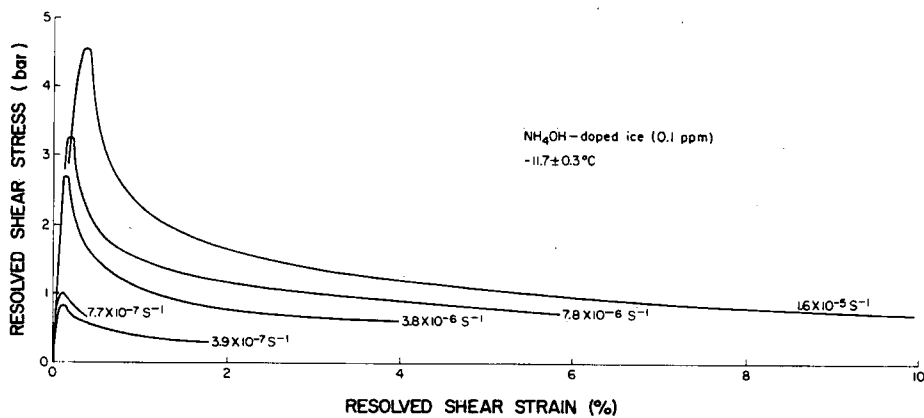


Figure 23. Stress-strain curves for NH₄OH-doped ice deformed at -11.7°C at various strain-rates as marked.

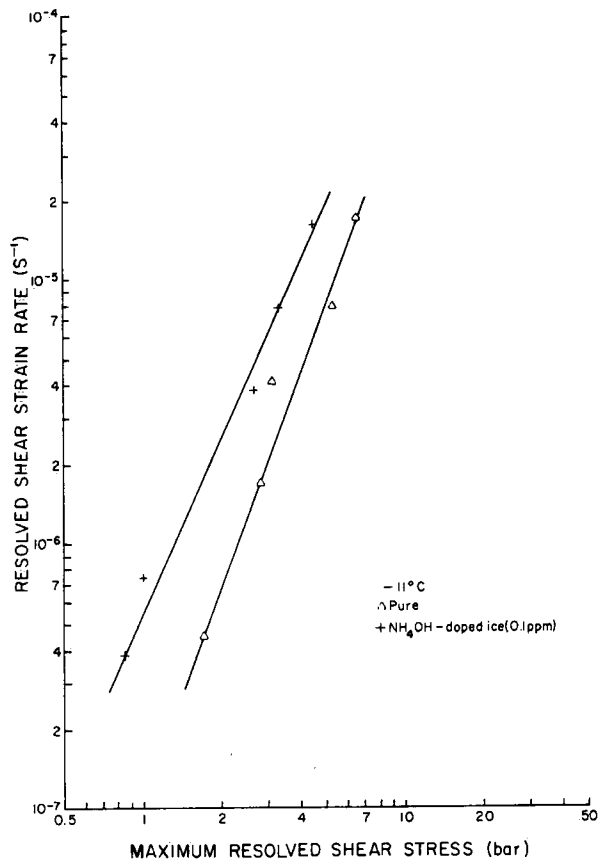


Figure 24. Maximum resolved shear stress plotted against strain-rate for pure and NH_4OH -doped ice at -11°C . The concentration of NH_4OH was about 0.1 ppm in the doped samples.

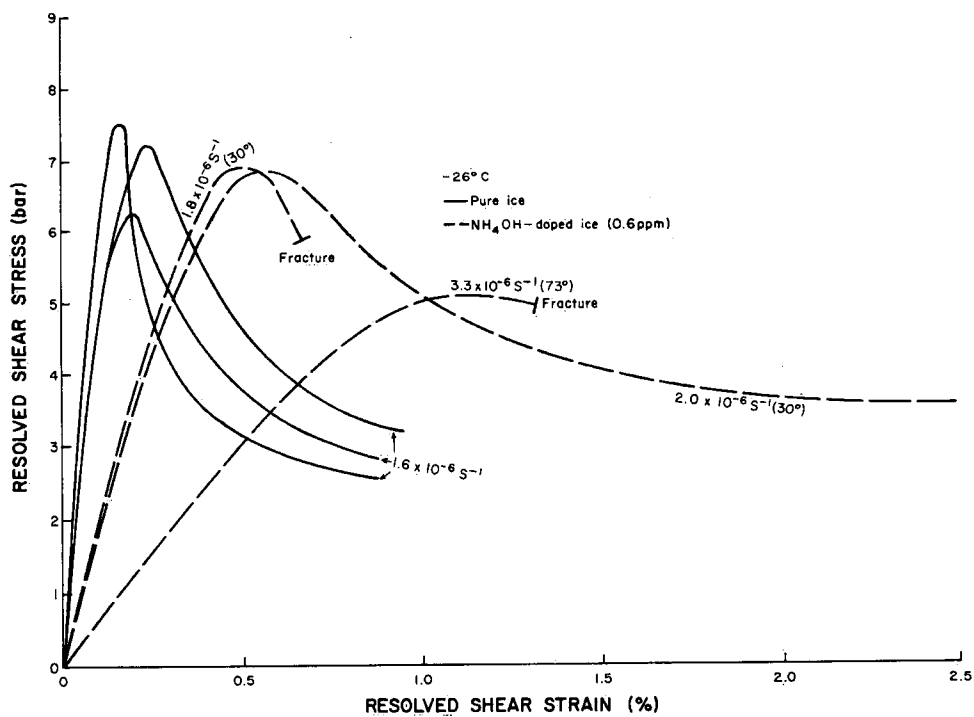


Figure 25. Stress-strain curves for NH_4OH and pure ice deformed at -26°C at various strain-rates as marked.

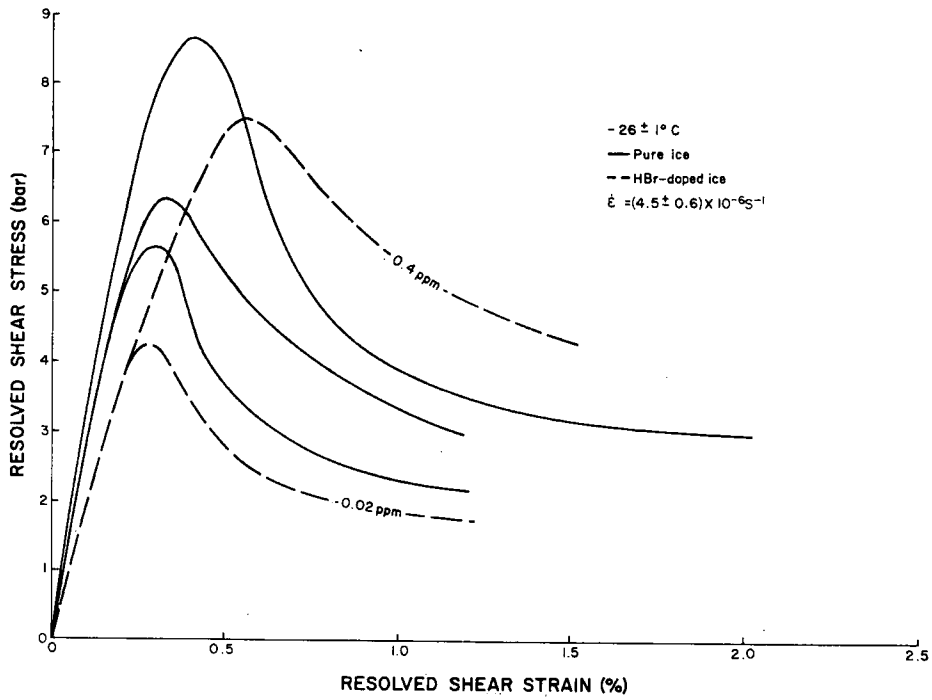


Figure 26. Stress-strain curves for HBr-doped ice deformed at -26°C at a strain-rate of 4.5 X 10⁻⁶ s⁻¹.

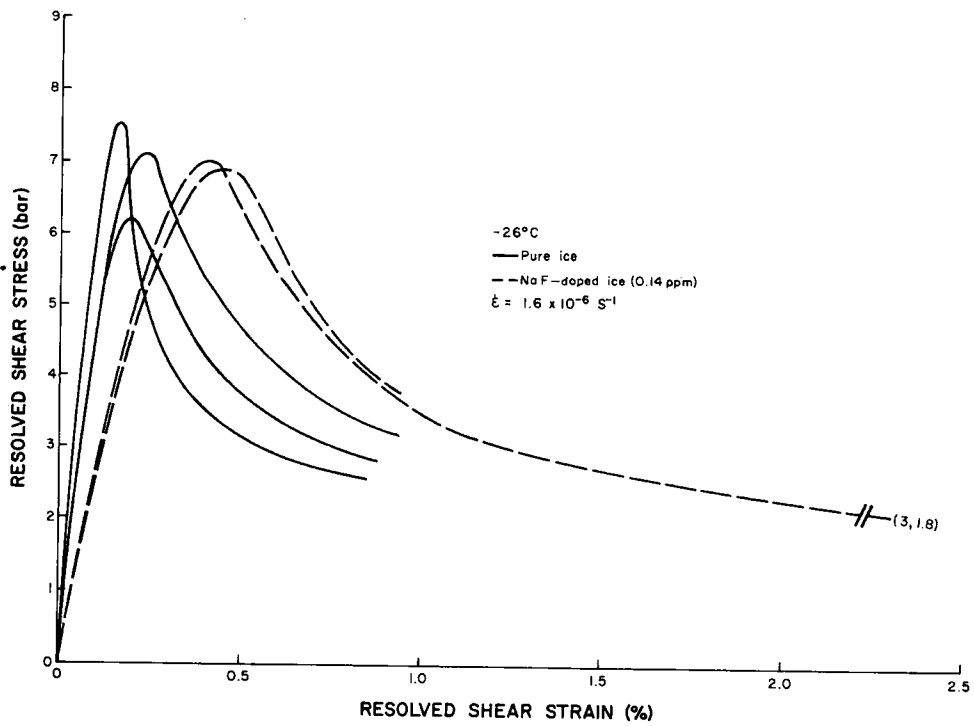


Figure 27. Stress-strain curves for pure and NaF-doped ice at -26°C at a strain-rate of 1.6 X 10⁻⁶ s⁻¹.

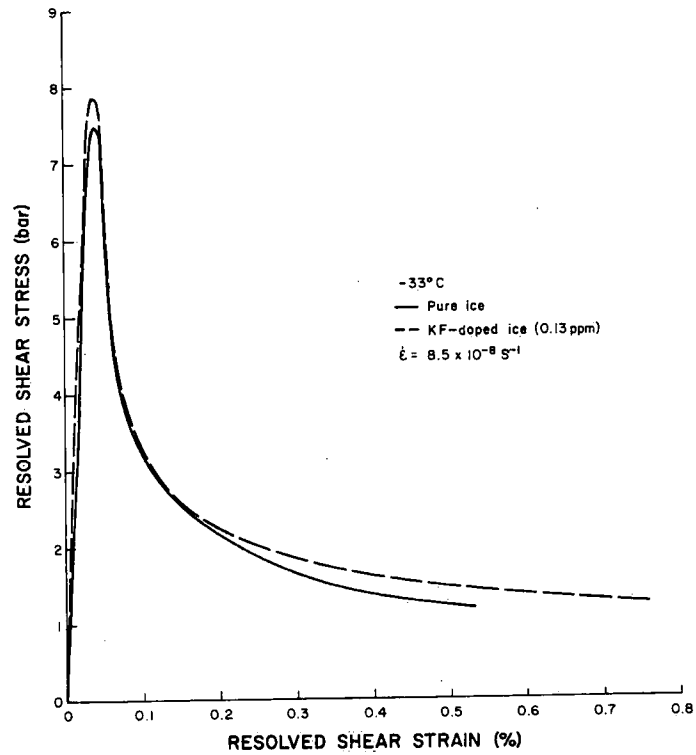


Figure 28. Stress-strain curves for one pure and one KF-doped sample deformed at -33°C and at a strain-rate of $8.5 \times 10^{-8} \text{ s}^{-1}$.

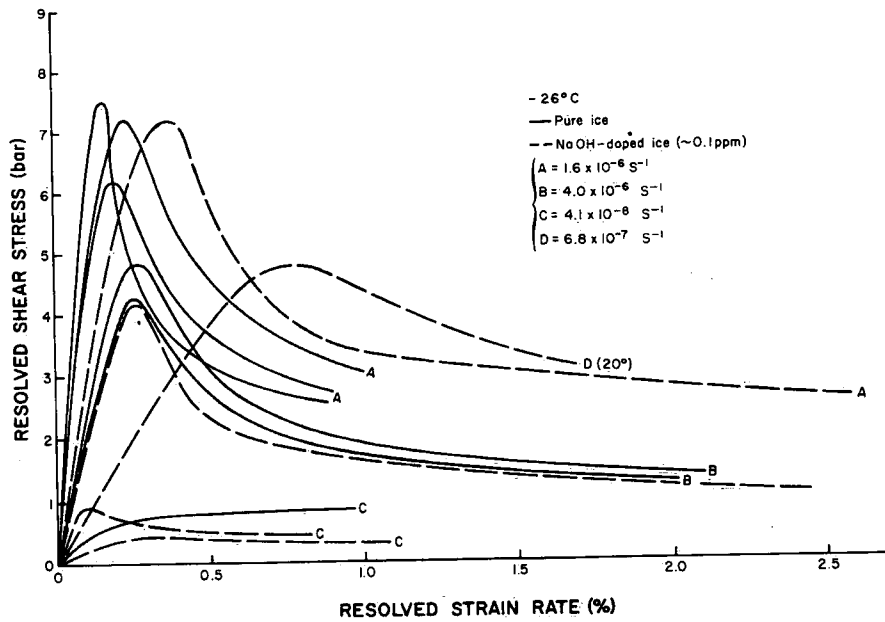


Figure 29. Stress-strain curves for pure and NaOH-doped ice deformed at -26°C at various strain-rates as marked on the figure. The curve marked D (20°) was a sample with an angle of 20° between its optic and tensile axis.

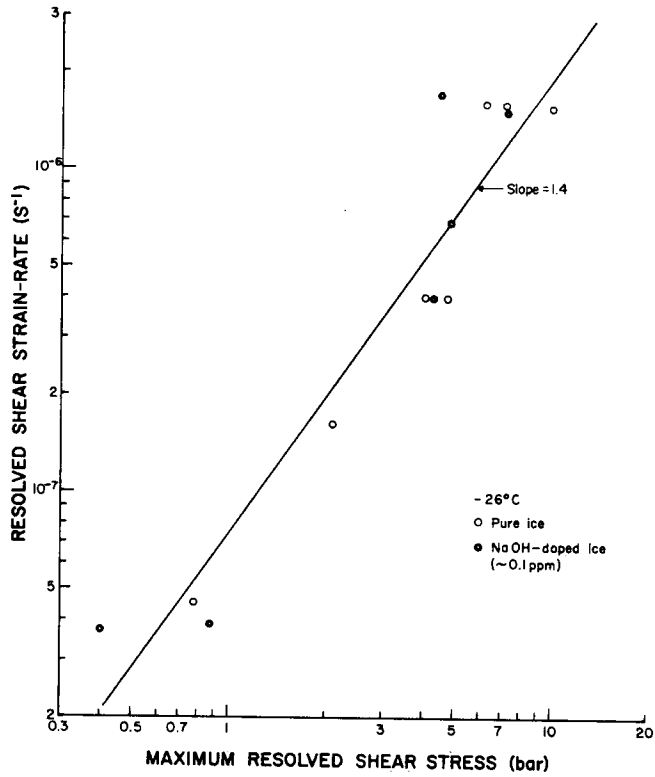


Figure 30. Maximum resolved shear stress plotted against strain-rate for pure and NaOH-doped ice at $-26^{\circ}C$.

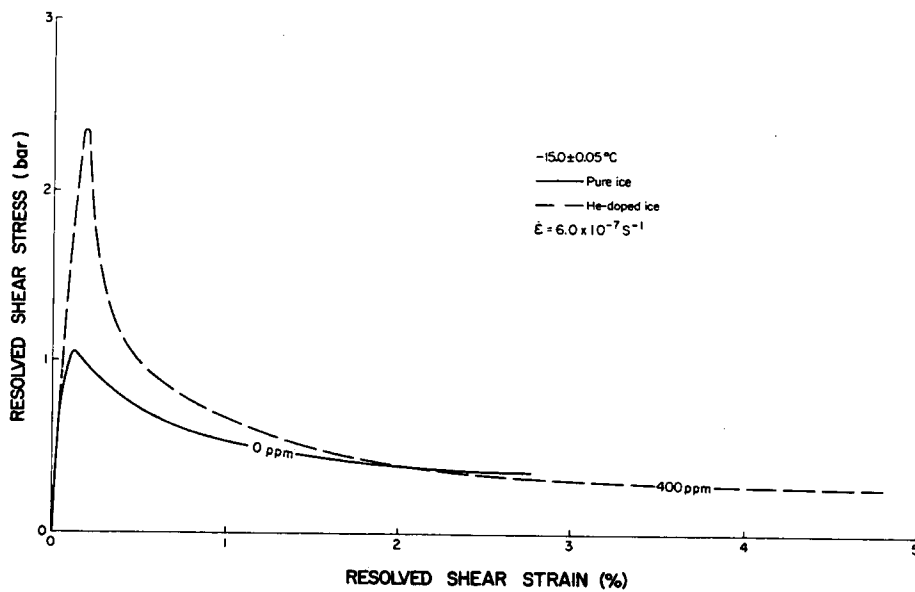


Figure 31. Stress-strain curve for two He-doped ice crystals deformed at $-15^{\circ}C$. After testing, one sample had no He left in it.

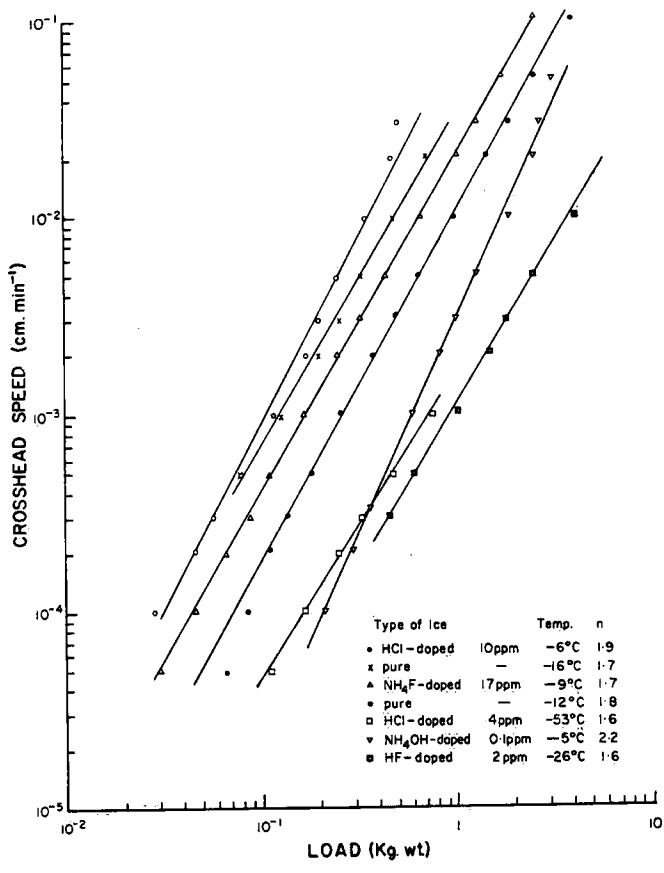
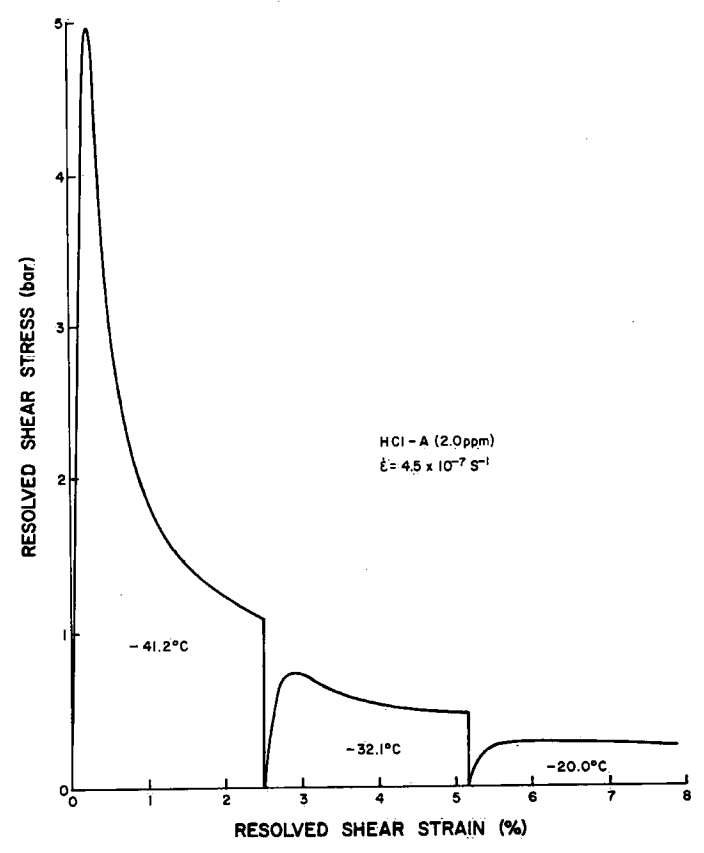


Figure 32. Showing the variation of load with crosshead speed. Each line represents one sample deformed at different rates at various temperatures down to -53°C . The slope of each line gives a stress exponent, n , shown in the figure.

Figure 33. Stress-strain curve for one HCl-doped specimen deformed at different temperatures at a strain-rate of $4.5 \times 10^{-7} \text{ s}^{-1}$



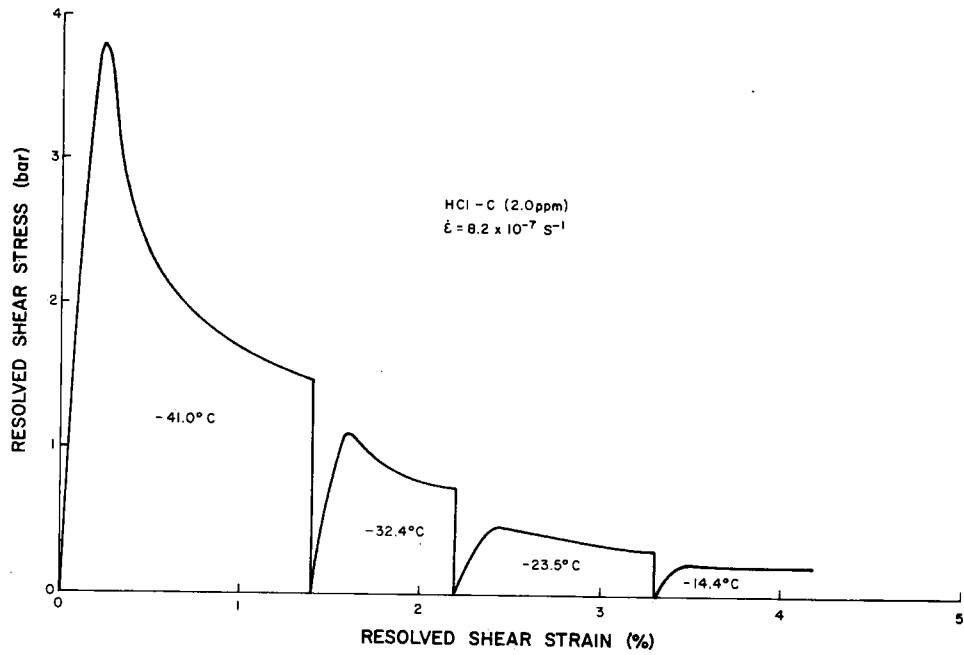


Figure 34. Stress-strain curve for one HCl-doped ice crystal deformed at different temperatures at a strain-rate of $8.2 \times 10^{-7} \text{ s}^{-1}$.

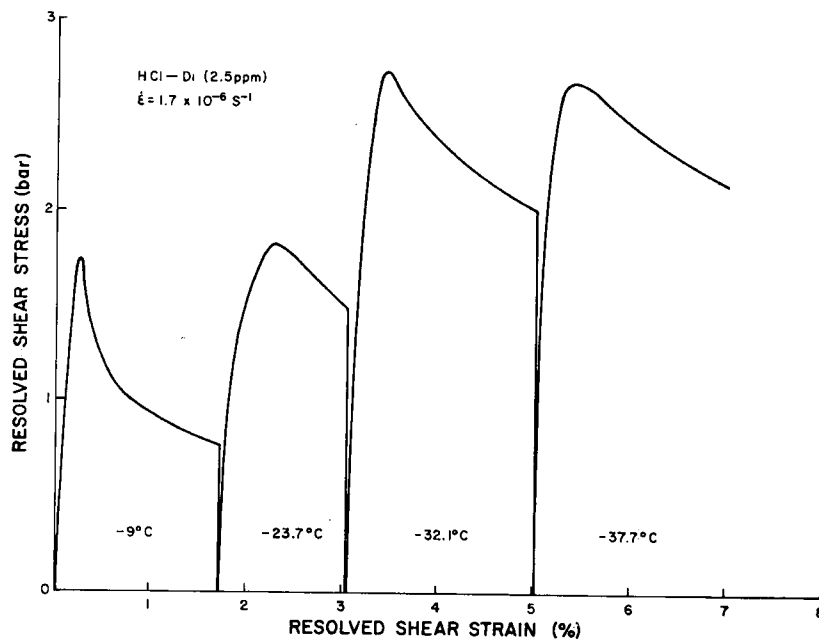


Figure 35. Stress-strain curve for one HCl-doped specimen deformed at different temperatures at a strain-rate of $1.7 \times 10^{-6} \text{ s}^{-1}$.

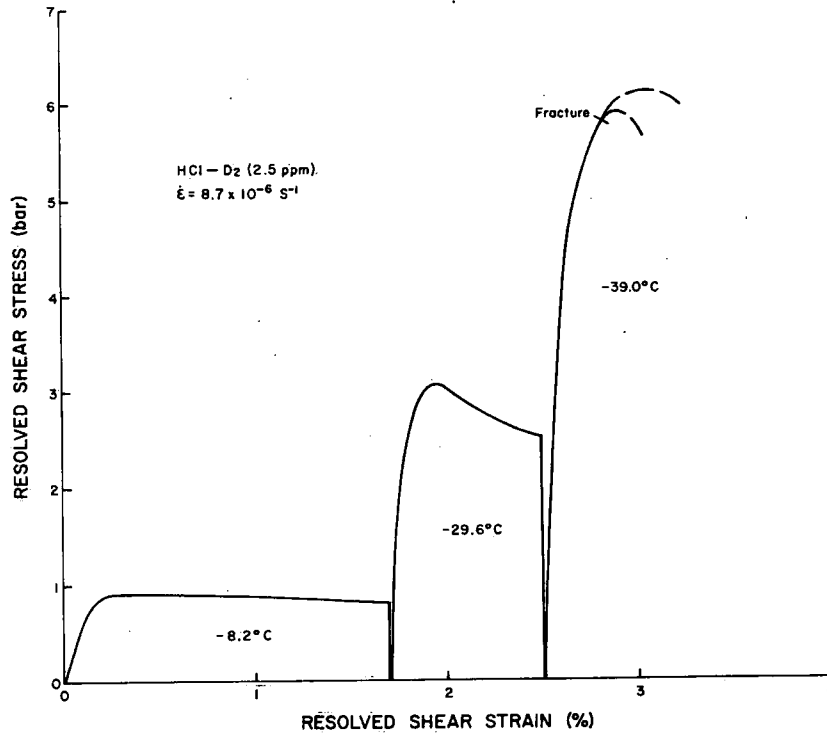


Figure 36. Stress-strain curve for HCl-doped specimen deformed at different temperatures at a strain-rate of $8.7 \times 10^{-6} \text{ s}^{-1}$. The sample was the same one as used for Figure 35.

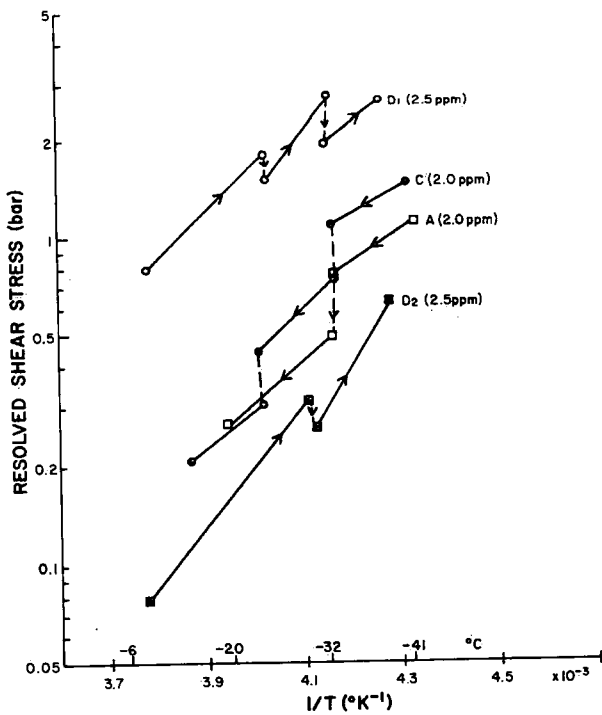


Figure 37. Determination of activation energy for HCl-doped crystals by comparison of stress immediately before and after changing temperatures. Samples used were those shown in Figures 33-36.

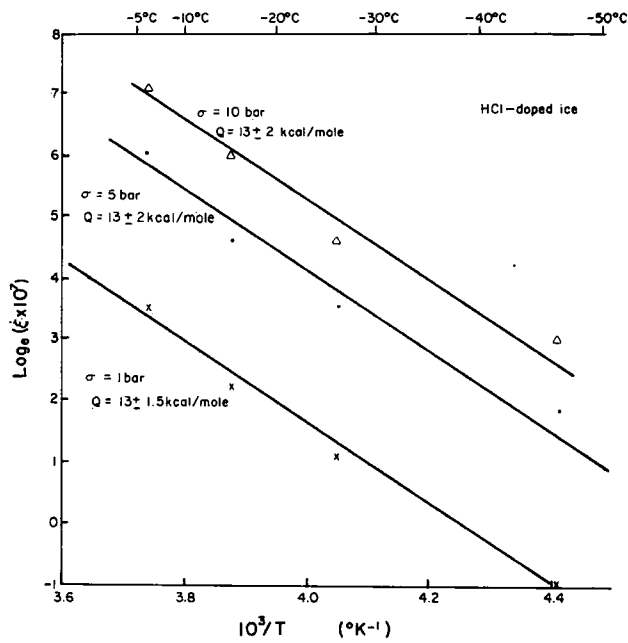
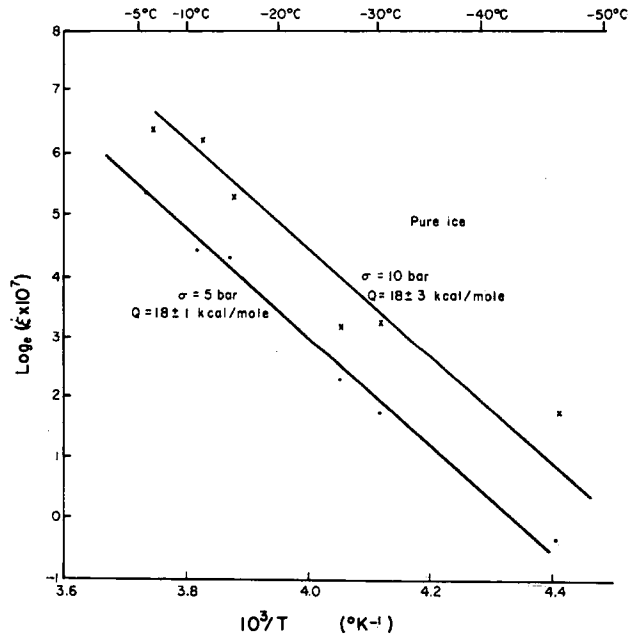


Figure 38. Determination of activation energy for HCl-doped ice by comparing strain-rates required at different temperatures to give a constant maximum resolved shear stress. Stresses are shown for each line and the slope of the line is proportional to the activation energy.

Figure 39. Determination of activation energy for pure ice by comparing strain-rates required at different temperatures to give a constant maximum resolved shear stress. Stresses are shown for each line and the slope of the line is proportional to the activation energy.



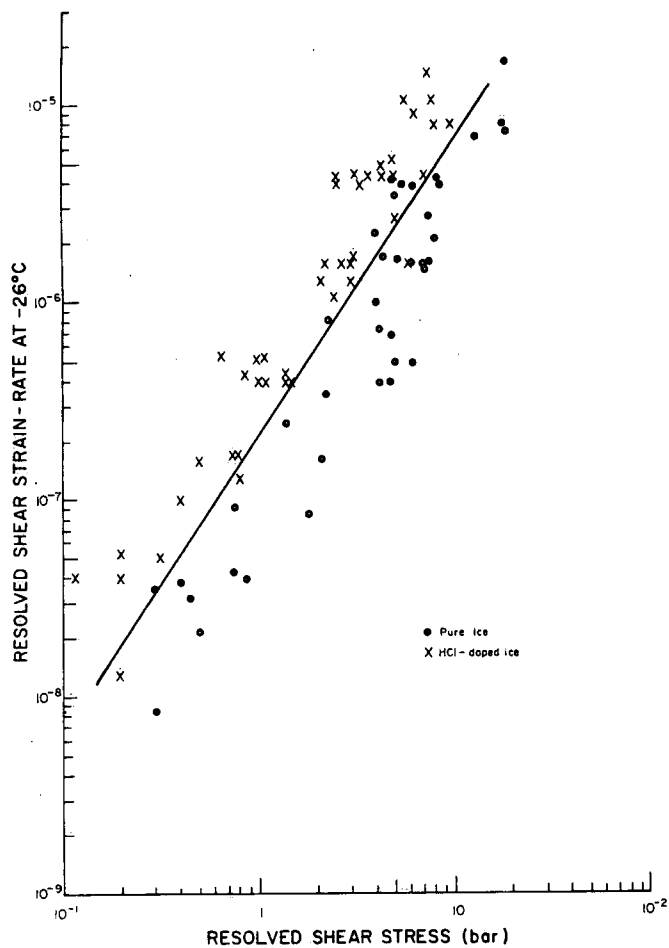
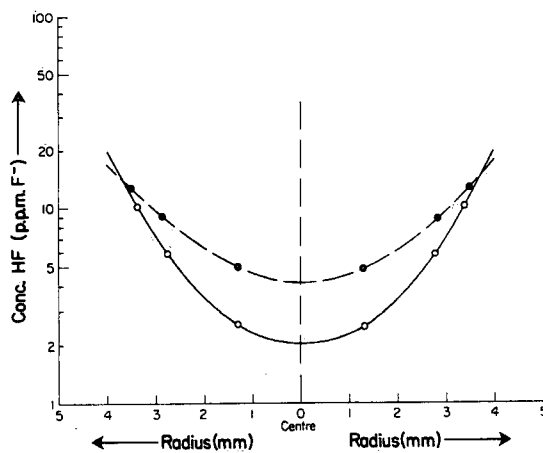


Figure 40. Maximum resolved shear stress for all pure and HCl-doped samples plotted against strain-rate reduced to -26°C by using an activation energy of 18 kcal/mole for pure ice and 13 kcal/mole for HCl-doped ice.

Figure 41. Radial distribution of fluoride in a cylindrical single crystal of HF-doped ice.



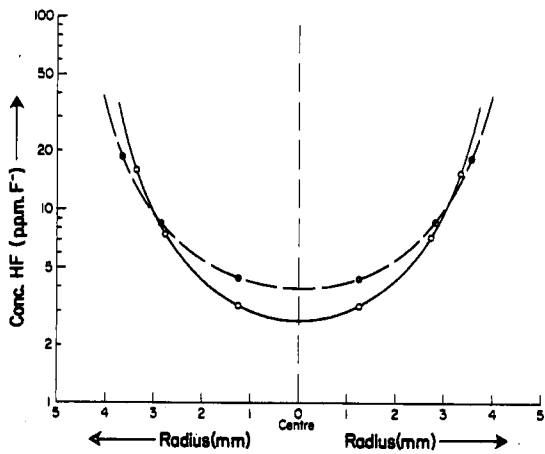


Figure 42. Radial distribution of fluoride ion in a cylindrical single crystal of HF-doped ice.

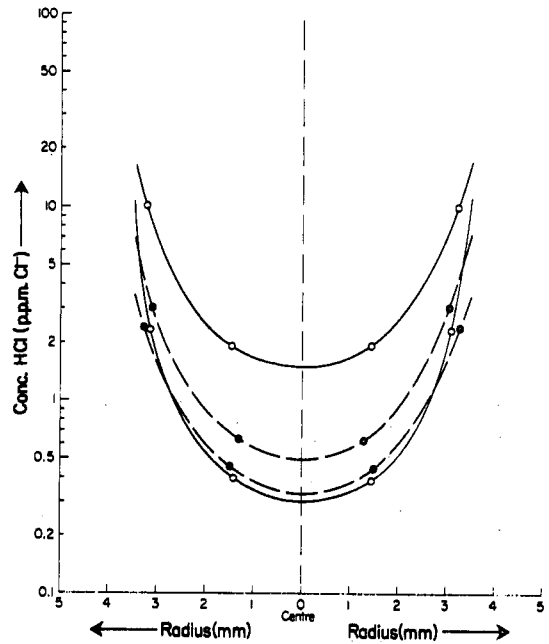


Figure 43. Radial distribution of chloride ion in a cylindrical single crystal of HCl-doped ice.

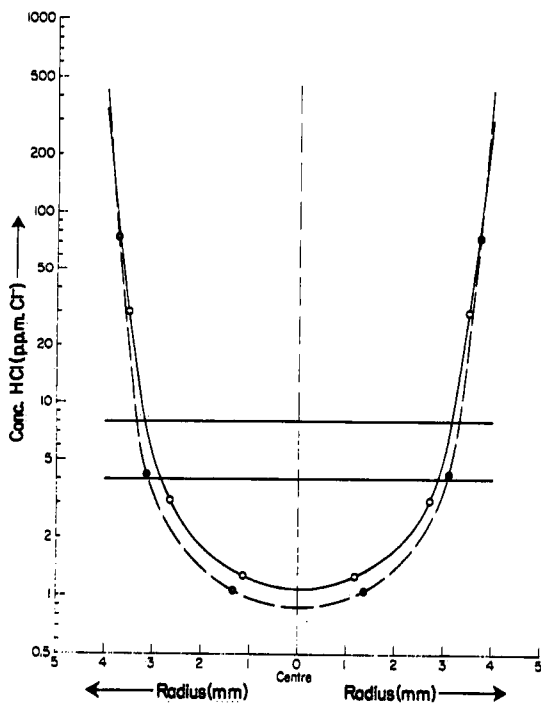


Figure 44. Radial distribution of chloride ion in a cylindrical single crystal of HCl-doped ice.

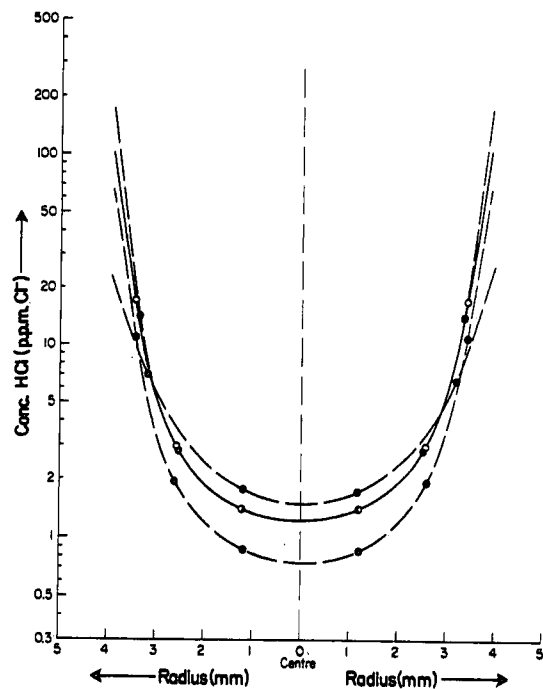


Figure 45. Radial distribution of chloride ion in a cylindrical single crystal of HCl-doped ice.

Environment Canada Library, Burlington



3 9055 1017 3262 5

